

Coral Species Replacements on Guam's Reef Flats: Investigating the Role of
Symbiodiniaceae Dynamics and Environmental Stressors

BY
CARLOS ALBERTO TRAMONTE

A thesis submitted in partial fulfillment of the
requirements for the degree of

MASTER OF SCIENCE

IN

BIOLOGY

UNIVERSITY OF GUAM

06/13/2023

AN ABSTRACT OF THE THESIS of CARLOS ALBERTO TRAMONTE for the
Master of Science in Biology presented, 06/13/2023

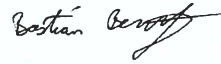
Title: Coral Species Replacements on Guam's Reef Flats: Investigating the Role of
Symbiodiniaceae Dynamics and Environmental Stressors

Approved:  _____

Dr. Bastian Bentlage, Chair, Thesis Committee

TO THE OFFICE OF GRADUATE STUDIES

The members of the committee approve the thesis of CARLOS ALBERTO TRAMONTE presented on 6/13/2023



Dr. Bastian Bentlage, Chair



Dr. Laurie Raymundo, Member



Dr. Sarah Davies, Member

ACCEPTED:

SJSantos-Bamba

SJSantos-Bamba (Jun 16, 2023 14:47 GMT+10)

Sharleen Q. Santos-Bamba, Ph.D.
Vice Provost for Graduate Studies

Jun 16, 2023

DATE

Abstract

On Guam, *Acropora pulchra* is being increasingly replaced by the stress tolerant/generalist agariciid coral *Pavona decussata* and the weedy coral *Pocillopora damicornis* via stress induced successional processes. In general, *Pavona decussata* and *Pocillopora damicornis* appear less susceptible to stressors relative to *Acropora pulchra*, potentially due to their Symbiodiniaceae associations, prompting the investigation of the potential mechanisms behind their differential stress susceptibility. Here we quantified coral-associated Symbiodiniaceae antioxidant response, photosynthetic dynamics, and community assemblages for 288 coral fragments across four timepoints, three species, two sites, and two reef zones within each site. Symbiodiniaceae photopigment and antioxidant dynamics were measured through the relative fluorescent intensities (RFI) of peridinin (Per), chlorophyll-a and chlorophyll-c₂ (Chl a/c₂), and flavin-based fluorescent proteins (FbFP). Symbiodiniaceae antioxidant associated responses were significantly different between *Acropora pulchra*, *Pocillopora damicornis*, and *Pavona decussata*, with *P. decussata* maintaining low levels of antioxidant associated RFIs across temporal and spatial scales. Our results also demonstrated distinct seasonal acclimatization patterns in photosynthetic associated RFIs across all species. In contrast to patterns observed in *Acropora pulchra* and *Pocillopora damicornis*, *Pavona decussata* displayed a divergent trend between photosynthetic associated RFIs and antioxidant associated RFIs, indicating a potential host-mediated photo-protective mechanism. This relationship may explain *P. decussata*'s increasing prevalence within reef flat communities, but, future work exploring this potential stress modulation is needed. We also found that coral associated Symbiodiniaceae communities were highly conserved across coral species and maintained high levels of uniformity across spatial scales, apart from Tanguisson Inner *Acropora pulchra*, which deviated from other *A. pulchra* Symbiodiniaceae assemblages. Our

results illustrated no observed differences in community composition shifts over temporal scales, however this is likely attributable to the relatively short duration of our observations. Our study highlights the complex adaptive strategies of *Acropora pulchra*, *Pocillopora damicornis*, and *Pavona decussata* in response to environmental stressors, offering insight into the mechanisms behind coral resilience and contributing to a deeper understanding of the factors shaping coral community composition shifts in Guam.

Acknowledgements

My Committee

I would like to begin by thanking my committee members Bastian Bentlage, Laurie Raymundo, and Sarah Davies, all of whom were instrumental to the success of this masters through personal and academic guidance. Sarah, I want to thank you for responding to my email all those years ago and letting me join your lab as an undergraduate. You took my curiosity in corals and elevated it to include a love for marine science, and with the help of Dan, Hannah, Nicola, James, and Hanny, you molded me into a budding scientist that got me to where I am today. I will forever appreciate you and your lab. Laurie, thank you for always being available to talk about my project. Your insight and questions are what got this project going in the first place, and I have loved being able to pick your brain about the complexity of this reef environment. Lastly, Bastian, you have been a helping hand for me as I turned this abstract idea of a project into a concrete and successful thesis. Your unwavering support and patience as I churned through this project is one that I look fondly on, and even more so I will miss our conversations and days spent in the field; hammering nails, getting bit by morays, and collecting samples as we fought against time so that we wouldn't get stuck on the reef flat during low tide. Thank you for everything you have done for me and for

challenging me to become a better scientist. You three are undoubtedly incredible, and I cannot begin express how grateful I am to have you all as mentors, professors, and friends in my life. I will always stay in touch as I continue my journey as a scientist and as a human being, thank you again for everything.

Mis padres

Gracias por ser unos padres excepcionales, maestros, amigos y consejeros, todo envuelto en unos seres humanos tan increíbles como ustedes. Su amor incondicional, apoyo incansable y sacrificios innumerables han sido fundamentales para llegar a donde estoy hoy. Sin su ayuda, nunca hubiera logrado todo lo que he alcanzado hasta ahora. Los amo muchísimo y son un verdadero ejemplo a seguir; me siento sumamente orgulloso y agradecido de poder decir que llevo en mi corazón y espíritu de vida sus esencias. Ustedes me han enseñado a luchar por mis sueños, a enfrentar las adversidades con valentía y a valorar la importancia de la perseverancia y la determinación. Sus corazones desbordan amor, generosidad y sabiduría, y me reconforta saber que siempre puedo contar con ustedes en cualquier situación, tanto en los momentos de alegría como en los desafíos más difíciles. A través de su guía y apoyo, han cultivado en mí la confianza y el coraje necesarios para perseguir mis metas y enfrentar los obstáculos que la vida me presenta. Es cierto lo que dicen: solo al crecer, comenzamos a comprender la magnitud del amor de nuestros padres y la profundidad de su entrega y sacrificio. Por todo esto y más, les estaré eternamente agradecido. De verdad, no tengo palabras suficientes para expresar mi gratitud y amor hacia ustedes. Gracias y un beso grande a los dos.

My friends and siblings

How do I even begin to thank you all for giving me a level of support and friendship that has shaped me into the individual I am today. All my friends, both on and off Guam, have

contributed to this journey, and I want to thank each and every one of you. First and foremost, I want to thank my friends from back home: Eduardo, Ferran, Dani, Hannah, Emi, Cheyenne, and Danny, for being at the foundation of my life. You have all grown up alongside me, sharing countless memories that will forever be etched in my heart. Your support and encouragement have been invaluable throughout the years, and as I complete my masters, I thank all of you for always being there for me when I need to hear familiar voices while being so far from home. To my college friends, Will, Alberto, Liz, Arsh, Rockib, Gaby, Arya, Fahad, Reggie, Jasmine, Grace, and Pao, thank you for enriching my academic and personal experience with your wisdom, laughter, love, and camaraderie. Our late-night and delirious study sessions, chem lab tomfoolery, dance practices, living room conversations, opening night movie runs, unforgettable weekends, and Boston/Australia adventures have left an indelible mark on my soul. Every one of you pushed me forward, getting me where I am today, and I thank you all for it. Special thanks to Will Trammell, who has been the best example of what being a best friend means, I'm with you till the end of the line, buddy. To my siblings, Gaby and Fio, I owe you both a debt of gratitude for being my greatest confidants, my fiercest protectors, and my most cherished companions. Your unwavering love and support, listening ears, and soothing words of reassurance have carried me through the most challenging times, getting me to where I am today. You both have been my rock and my inspiration, and for that and more, I am proud to call you both, family. To my friends in Guam, thank you for making my time here on this seemingly endless summer an absolute blast. I don't think there will ever be a place as spectacular as Guam, and I feel like a lot of that is due to all of you. I will always remember our spike ball sessions, water polo games, poker nights, Hilaan hammock sessions, and endless dives and hikes. You have all enriched my life, broadened my perspectives, and taught me all so much as I completed my thesis. I am grateful for the connections

we have forged, and I will treasure the memories we've created together very fondly. I'd like to give an incredibly special thanks to Marisa Agarwal, I am so happy to have been able to experience this island with you and watch the sunset cast so many paintings in the sky. You have helped me so many times in the field, in the lab, and in my analysis that my success in completing my masters is in large part because of you (without you, I would still be struggling to make a simple bar plot in R haha). You have made me grow intellectually, emotionally, and academically, and I can't thank you enough for what you have brought to my life.

Marine Lab and UOG

I am immensely grateful for all the staff, faculty, and students of the UOG Marine Lab for all your support during my project. A very special thanks is deserved to techs Nanny, Jay, and John for their friendship, laughs and for always lending a helping hand regarding my little '96 Honda Acty. I'd also like to give a special thanks to Colin Lock, Colin Anthony, Ginger Carter, and Olivia Barry for helping me with field work and getting me up and running in the lab. Additionally, thank you to the EPSCoR team for creating a friendly and inviting atmosphere whenever I asked for help, it was so appreciated, and you all do incredible work to support all of us here at the Marine Lab.

This material is based on work supported by the National Science Foundation Award No. OIA1457769, Guam Ecosystems Collaboratorium for Corals and Oceans (GECCO).

Table of contents

Abstract

Acknowledgments

1.0 INTRODUCTION.....	16
1.0.1 Problem Statement	
1.1 Ecological Succession.....	17
1.2 Coral Bleaching on Guam.....	18
1.3 Coral-Symbiodiniaceae Mutualism & Diversity	19
1.4 Symbiodiniaceae Photophysiology and Photobiochemistry.....	21
1.4.1 Peridinin and Chlorophyll	
1.4.2 Xanthophylls, Diatoxanthin, and β -carotene	
1.4.3 Flavoproteins	
1.5 Key Ecosystem Engineers on Guam’s Reef Flats.....	25
1.5.1 <i>Acropora pulchra</i>	
1.5.2 <i>Pocillopora damicornis</i>	
1.5.3 <i>Pavona decussata</i>	
1.6 Coral Species Replacement.....	28
1.7 Abiotic Factors that Shape Guam’s Reef Flats.....	30
1.7.1 Vertical Tectonic Motion	
1.7.2 Tidal Exposure	
1.7.3 Water Flow Dynamics	
1.8 Research Questions.....	32

1.8.1 Null and Alternative Hypotheses	
1.9 MATERIALS AND METHODS	33
1.9.1 Study Location	
1.9.2 Ecological & Environmental Monitoring	
1.9.3 Field Collection	
1.9.4 Symbiodiniaceae Biodiversity	
1.9.5 Symbiodiniaceae Density & Autofluorescence	
2.0 Statistical Analysis	41
2.1 RESULTS	42
2.1.1 Environmental Factors	
2.1.2 Ecological Monitoring	
2.1.3 Symbiodiniaceae Community Diversity	
2.1.4 Symbiodiniaceae Densities & Autofluorescence	
2.2 DISCUSSION	46
2.2.1 Reef Community Stability	
2.2.2 Symbiont Community Diversity & Structure	
2.2.3 Symbiodiniaceae Autofluorescent Dynamics	
2.2.4 Symbiodiniaceae Densities	
2.3 Conclusions	54
2.4 References	70
Appendix	

List of Tables

Table 1: Series of Repeated Measures - MANOVAs determining *which factors* contributed to physiological variation *in cellular density, peridinin, chlorophyll, and antioxidant associated RFI*, over time, site, zone, *and* species.

Table 2: Series of Kruskal-Wallis nonparametric tests to determine contributions to Ecological Monitoring data via time, site, zone, benthic component, and non-coral vs coral comparisons; Temperature data via time, site, and zone; and Rainfall data via time comparisons. Contributions to Current Speed data were discovered using ANOVAs via time, site, and zone comparisons.

Table 3: Series of Pairwise Adonis for Symbiodiniaceae ITS2 Types.

Table 4: Series of Pairwise Adonis for Symbiodiniaceae ITS2 Types.

Table 1A. Peridinin – Chlorophyll LHC linear models specific to site, species, and time.

List of Figures

Figure 1: Phylogenetic tree of Symbiodiniaceae family. *Symbiodinium*, *Breviolum*, *Cladocopium*, and *Durusdinium* being closely related to corals (Diagram taken from LaJeunesse et al., 2018).

Figure 2: Xanthophyll, carotenoid, and β -carotene pathway in the PS-II, illustrating quenching and subsequent stress signaling (Diagram taken from Swapnil et al., 2021).

Figure 3: 2011-2020 mean percent bleaching and mortality for three coral families. Acroporidae, Agariciidae and Pocilloporidae abundance values correlated with the mean percent (%) affected in terms of bleaching and mortality across West Agaña and Tanguisson from 2011-2020 (Data taken from Raymundo et al., *in prep*).

Figure 4: Tanguisson (A) and West Agaña (B) field site with six 15m fixed transect tapes rolled out parallel to shore for inner and outer zones (A1, B1, B2).

Figure 5: 2013–2017 time series of running 7-d mean sea surface temperature (SST) from the NOAA CRW virtual station for Guam plotted against annual maximum monthly mean SST (AMMM), bleaching threshold (BT), and degree heating weeks (DHW) for 2013–2017 (Diagram taken from Raymundo et al., 2019). Coral samples were collected at four different timepoints.

Figure 6: Experimental design; illustrating two sites (Tanguisson and West Agaña), each with two treatments (inner and outer zone) and three transects per treatment zone. Within each transect, two *A. pulchra*, *P. damicornis*, and *P. decussata* were tagged and sampled across four timepoints.

Figure 7: a). Symbiodiniaceae forward + side scatter to calculate cell densities via Guave easyCyte Flow Cytometer wavelength lasers and 3D mesh model used to normalize Symbiodiniaceae cell counts. **b).** (BLUE BAND): Per and antioxidant associated pigment excitation at 488 nm via the blue laser. Green, Yellow, and Red filters used to determine specific pigments **c).** (RED BAND): Chl *a/c*₂ excitation at 642 nm via the red laser and red filtration. (Diagram taken from Anthony et al., 2022).

Figure 8: a) Mean daily sea surface temperatures (SST) for each site zone captured by Onset HOBO temperature loggers across 12-month period (February 2022-2023) overlaid with precipitation data from the same period collected by Menne et al., 2012. Sample collections were completed in February (blue, pre-warming period), May (yellow, transitional pre-warming period), August (orange, peak warming period), November (light blue, transitional post-warming period), and are shown by the blue, yellow, orange, and light teal bars. **b)** Distribution of mean daily SSTs across the 12-month period (February 2022-2023) illustrating differences in extremes between Inner and Outer zones for each site.

Figure 9: a) Mean daily current speed (cm/s) for each site and zone captured by TCM-4 Shallow water Tilt Current Meters across a 3-month period (December 2022-February 2023). **b)** Distribution of mean daily current speed (cm/s) across 3-month period (December 2022-February 2023) illustrating differences in extremes between the inner and outer zones for each site.

Figure 10: Stacked bar plot showing percent coverage of benthic components across site zones: *Acropora pulchra* (*A. pulchra*), *Pocillopora damicornis* (*P. damicornis*), *Pavona decussata* (*P. decussata*), Other coral species (Other), Algae, and Non-Living Substrate. Surveys were conducted in February (pre-warming period) and August (peak warming period).

Figure 11: Photographs taken of tagged **a)** *Acropora pulchra*, **b)** *Pocillopora damicornis*, and **c)** *Pavona decussata* coral colonies during ecological monitoring surveys in February (pre-warming period) and August (peak warming period).

Figure 12: a). *ITS2* type and type profile diversity for coral associated Symbiodiniaceae found within tagged *Acropora pulchra*, *Pocillopora damicornis*, and *Pavona decussata* colonies for each site and zone across time.

Figure 13: Symbiodiniaceae densities (cells/cm²) for *Acropora pulchra*, *Pocillopora damicornis*, and *Pavona decussata* in February (pre-warming period), May (transitional pre-warming period), August (peak warming period), and November (transitional post-warming period) for Tanguisson (blue) and West Agaña (orange). Points represent average RFI contributions for each colony collected. Stars represent significance level.

Figure 14: Symbiodiniaceae Relative Fluorescent Intensity (RFI) for antioxidant associated fluorescent proteins. Samples were analyzed from tagged *Acropora pulchra*, *Pocillopora damicornis*, and *Pavona decussata* colonies that were collected in February (pre-warming period),

May (transitional pre-warming period), August (peak warming period), and November (transitional post-warming period) for Tanguisson (blue) and West Agaña (orange). Points represent average RFI contributions for each colony collected. Stars represent significance level.

Figure 15: Peridinin – chlorophyll associated RFI ratios for *Acropora pulchra* (yellow), *Pocillopora damicornis* (blue), and *Pavona decussata* (pink) across February (pre-warming period), May (transitional pre-warming period), August (peak warming period), and November (transitional post-warming period) for sites and zones. Linear regression equations indicate peridinin – chlorophyll ratios, while dotted lines indicate 1:1 relationship for reference.

1.0 INTRODUCTION

1.0.1 Problem Statement

As global sea surface temperatures persistently rise, the frequency and severity of coral bleaching and mortality events have increased, posing a significant threat to coral ecosystems (Hoegh-Guldberg, 1999, Hoegh-Guldberg and Smith, 1989; Sully et al., 2019). Guam's reefs exemplify this trend, with a staggering 36% decrease in coral cover between 2012 and 2017, predominantly due to *Acropora pulchra* mortality in reef flat communities (Raymundo et al., 2017, 2019). As a crucial habitat-forming ecosystem engineer, *Acropora pulchra* plays a vital role in enhancing fish biodiversity and mitigating wave action (Johnson et al., 2011; Kuffner & Toth, 2016). Over the past decade, however, field observations have detailed *Acropora pulchra* being increasingly replaced by the generalist/stress tolerant agariciid coral *Pavona decussata* and the weedy coral *Pocillopora damicornis* via successional processes. This community-level shift has led to pronounced changes across the nearshore and farshore zones of Guam's reef flats, dynamics potentially exacerbated by successive disturbance events and influenced by water flow dynamics (Anthony & Kerswell, 2007; Johansen, 2014; Fifer et al., 2021). Generally, *Pavona decussata* and *Pocillopora damicornis* exhibit lower susceptibility to disturbances than *Acropora pulchra* (Berg et al., *In Prep*; Lock et al., *In Prep*), necessitating an investigation into the underlying causes and mechanisms responsible for their differential stress susceptibility. A critical factor in coral stress susceptibility are the Symbiodiniaceae assemblages harbored within coral tissues (Berkelmans & van Oppen, 2006; Hoegh-Guldberg et al., 2007; LaJeunesse et al., 2018). By examining the variations in Symbiodiniaceae communities and their functional characteristics, we may unlock crucial insights into the successional dynamics of coral community composition shift observed on Guam's reef flats and contribute to a more comprehensive understanding of coral resilience in the face of increasing environmental stressors.

1.1 Ecological Succession

Succession is a fundamental ecological process defined as predictable community development toward a stabilized climax stage (Odum, 1969) that is most notable in its function of recovery following disturbances (Connell & Slatyer, 1977; Sandin & Sala, 2012; Buma et al., 2017). However, ecosystems can either exist as a stable climax state when uninterrupted (Connell & Slatyer, 1977), or in a constant unstable state if frequently impacted by stressors or disturbance events (Connell & Slatyer, 1977; Sandin & Sala, 2012). Even so, these different states do not always reflect the overall health of an ecosystem, as unstable states can be indicators of both unhealthy or healthy ecosystems (Connell, 1978; Griggs, 1983). This constant instability within high biodiversity ecosystems highlights how the severity of a disturbance event is more influential than whether a disturbance event occurs or not (Connell, 1978; Griggs, 1983). These disturbance events are one of the main contributors to ecological change, and as such, drive the different types and models of ecological succession.

Two major types of ecological succession occur in nature: primary and secondary succession. Primary succession is characterized by the colonization of a species onto a completely novel environment never inhabited by other species. In contrast, secondary succession defines itself as a replacement of flora and fauna after a disturbance event in a previously established environment (Walker & del Moral, 2003). Succession can be further broken down into three different models: facilitation, tolerance, and inhibition (Connell & Slatyer, 1977). The facilitation model dictates that later successional species are successful in their growth because early successional species modify the environment enough to make it favorable for later successional species. The tolerance model suggests that early successional species neither increase nor decrease later successional species growth and maturity, but rather, that different life history strategies are the main contributors to an ecosystem's succession. These different life-history strategies allow one

successional species to exploit a resource, with later successional species tolerating lower levels of a resource to survive. This tolerance allows later successional species to grow and succeed within the presence of an early successional species. The inhibition model postulates that the only reason later successional species grow and succeed is because early successional species die off or are damaged by a disturbance event, allowing limiting resources like space and energy to be released. If early successional species are not disturbed, then they will continue to occupy space and resources, preventing later successional species from succeeding. Given this, the three successional models (facilitation, tolerance, inhibition) provide a framework for what may be occurring on Guam's reef flats. Since corals operate within an ecological space, looking at the complexity of succession is imperative in understanding its effects on coral reefs.

1.2 Coral Bleaching on Guam

Coral reefs provide a myriad of functions: they support 25% of all marine life, provide food security and economic well-being for humans, and protect coastal areas from wave action, erosion, and tropical storms (IPCC Special Report, 2021). Climate change has threatened these functions, and now more than 50% of coral reefs are at medium or high risk of degradation and coral bleaching (Burke et al., 2011). Coral bleaching involves the breakdown of the relationship between a coral host and its photobiont in the Family Symbiodiniaceae (Glynn, 1984; Hoegh-Guldberg, 1999, 2017, LaJeunesse et al., 2018). This breakdown is recognized by distinct paling and complete color loss in corals due to the expulsion of Symbiodiniaceae (Hoegh-Guldberg, 1999), which can lead to increased mortality and disease susceptibility (Hoegh-Guldberg, 1999; Eakin et al, 2010; Muller, 2018; Rodgers, 2017). Although the bleaching of individual coral colonies has been reported for nearly ninety years (Yonge and Nichols, 1931), worldwide increases in the magnitude and severity of bleaching events in the last thirty years have reduced the biodiversity

and function of reefs globally (Hoegh-Guldberg, 1999, 2017; Hughes et al., 2017b). Sea surface temperatures (SST) throughout the tropics have increased by approximately 1°C in the last century, with current estimates placing future increases at around 1-2°C per century (IPCC 2021). Rising SST has a negative direct effect on coral reefs around the world (Hoegh-Guldberg, 1999, Hoegh-Guldberg and Smith, 1989; Sully et al., 2019), and the island of Guam is no different (Raymundo et al., 2017; Raymundo et al., 2019). Guam's forereefs and reef flats have had a coral cover reduction of nearly 36% from 2012 to 2017, with *Acroporidae* populations decreasing by nearly 50% from 33.3 to 17.8 ha from 2013 to 2015, primarily due to increased SST, extreme low tides, and disease (Raymundo et al., 2017, 2019). Additionally, disruptions in El Niño Southern Oscillation (ENSO) patterns and marine heatwaves likely exacerbated Guam's 2013, 2014, 2016, and 2017 bleaching events (Raymundo et al., 2017; 2019). However, as bleaching events increase in severity and frequency, we must not only focus on the ecological and ecosystem functions of a reef system, but also fundamentally understand the host symbiont interactions found within *Acropora pulchra*, *Pocillopora damicornis*, and *Pavona decussata*.

1.3 Coral-Symbiodiniaceae Mutualism & Diversity

Corals and Symbiodiniaceae form unique symbiotic assemblages within the coral host, creating diverse ecological communities (Wepfer et al., 2020). This interaction is based on a mutualistic nutrient exchange whereby corals rely on Symbiodiniaceae for carbon and nitrogen fixation and Symbiodiniaceae rely on the coral host for metabolic byproducts (Muscatine et al., 1984; Ezzat et al., 2017; Baker et al., 2013; Matthews et al., 2017; Hughes et al., 2017a; Vega Thurber et al., 2014). The mutualistic interaction between the coral host and diverse Symbiodiniaceae genera are inherently linked to the health and success of reef-building corals; their success is attributable to both organisms supporting each other's energy requirements

(Muscatine & Porter, 1977). Symbiodiniaceae communities can be shaped by many factors, such as coral host species (Baker, 2003), geography (LaJeunesse et al., 2004), depth (Sampayo et al., 2007), habitat (LaJeunesse et al., 2010a), light availability (Rowan, Knowlton, Baker, & Jara, 1997), and temperature (LaJeunesse et al., 2010a). This mutualism also determines coral susceptibility to heat stress and bleaching, which can be dependent on the specific Symbiodiniaceae clade that the coral hosts (Berkelmans & van Oppen, 2006; Hoegh-Guldberg et al., 2007; LaJeunesse et al., 2018).

Symbiodiniaceae have greater morphological and genomic variation than previously recognized, which has led to the description of several new genera and species (LaJeunesse et al.,

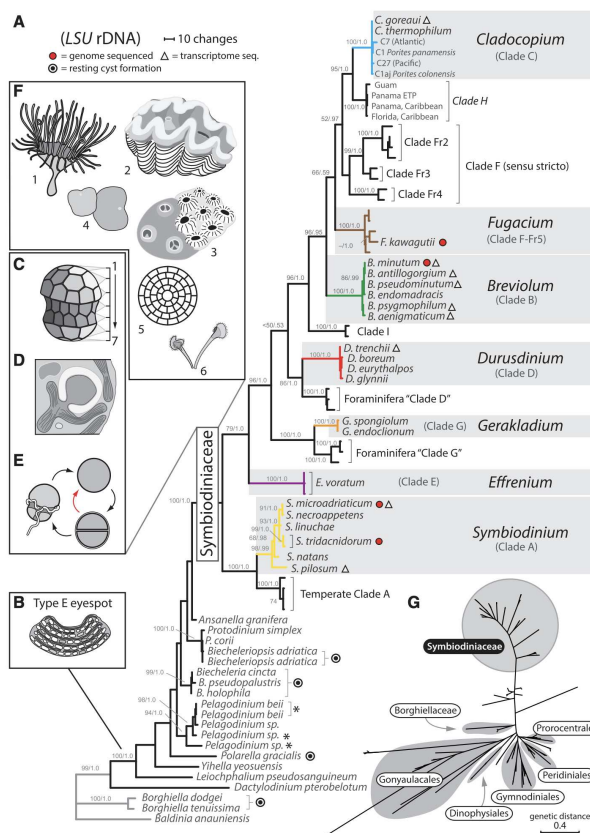


Figure 1: Phylogenetic tree of Family Symbiodiniaceae family. *Symbiodinium*, *Breviolum*, *Cladocopium*, and *Durusdinium* associated more commonly with corals (Diagram taken from LaJeunesse et al., 2018).

2018; Rowan and Powers, 1991, 1992). Seven genera of Symbiodiniaceae are currently described (Figure 1), and each can exhibit different physiological characteristics that impact thermotolerance and host nutrient provisioning, creating distinct coral holobiont assemblages (LaJeunesse et al., 2018; Berkelmans & van Oppen, 2006; Grégoire et al., 2017). The Symbiodiniaceae genera that are most distinctly associated with corals include *Symbiodinium* (previously Clade A), *Breviolum* (previously Clade B), *Cladocopium* (previously Clade C), and *Durusdinium* (previously Clade D) (Baker et al., 2013; LaJeunesse et al., 2018). The two most

common Symbiodiniaceae genera in the Pacific are *Cladocopium* and *Durusdinium* (LaJeunesse, 2005). *Cladocopium* possesses a generalist life history strategy, where there is a balance between thermotolerance and carbon and nitrogen fixation (Baker, 2003; LaJeunesse et al., 2018). *Durusdinium*, by contrast, tends to be found in highly variable light and temperature environments (Oliver & Palumbi, 2011; Silverstein et al., 2017) and can be associated with higher thermotolerance limits. However, this resilience comes with the tradeoff of decreased carbon and nitrogen fixation in their host, which may decrease the physical growth of the coral (Baker, 2003; LaJeunesse et al., 2018; Berkelmans & van Oppen, 2006). It has also been shown that *Cladocopium* and *Breviolum* harbor numerous host-specific phylotypes that each may have distinct functional roles across coral species (LaJeunesse et al., 2018), with some phylotypes potentially having higher tolerances than others (Widiastuti et al., 2015). This differs from *Durusdinium* and *Symbiodinium*, which are more opportunistic specialists and generalists that can allow their coral host to survive across a broad range of environments, reduce bleaching, and increase survival during peak thermal extremes (Jones et al., 2008; Berkelmans & van Oppen, 2006). As such, understanding functional variations in thermal tolerance, light-tolerance, and nutrient provisioning of Symbiodiniaceae is integral in disentangling potential drivers of large-scale community composition shifts on Guam's reef flats.

1.4 Symbiodiniaceae Photophysiology and Photobiochemistry

1.4.1 Peridinin and Chlorophyll

Terrestrial plants harbor photosynthetic pigments that capture photons, driving oxygenic photosynthesis (Büchel, 2020; Jiang et al., 2014; Bautista et al., 1999b). Photosynthetic dinoflagellates, such as Symbiodiniaceae, are no different. However, dinoflagellates contain different light-harvesting pigments (Falkowski and Raven, 1997), leading to differences in their

photosynthetic apparatuses. These membrane-bound apparatuses attach chlorophylls (Chl) and carotenoids (Car) via non-covalent interactions, creating a light-harvesting complex (LHC) (Kühlbrandt et al., 1994) made up of Car and Chl. Additionally, unlike terrestrial plants, Symbiodiniaceae possess Chl *a* – Chl *c*₂, but not Chl *b*. Similarly, to Chl subgroups, Cars can be divided into carotenes and xanthophylls, of which the latter are broken up into subgroups including fucoxanthin (Fx) and peridinin (Per). Fx and Per also have slightly different molecular structures (Büchel, 2020) and can form fucoxanthin-Chlorophyll-Protein Complexes (FCP) and Peridinin-Chlorophyll-Protein Complexes (PCP) (Norris and Miller, 1994). Furthermore, Symbiodiniaceae utilize two different LHCs: PCP as well as the Chl *a* - Chl *c*₂-peridinin protein complex (acpPC) (Polívka et al. 2007; Hiller et al. 1993). These complexes often have equal or higher Car to Chl ratios in dinoflagellates, and are the predominant complex in Symbiodiniaceae. Hofmann et al. (1996) showed that the dinoflagellate *Amphidinium carterae* displayed a Car to Chl ratio of 4:1, signifying the importance of Car as light harvesting pigments (Hofmann et al., 1996). The Per and Chl absorption spectra are found between 400-500nm and at 450 and 630nm (Büchel, 2020; Fawley, 1989), respectively, with high levels of excitation energy transfer between the Per and Chl (Hiller et al., 1993; Polívka et al., 2006; Iglesias-Prieto et al., 1993; Bautista et al., 1999b; Song et al., 1976). The excitation energy in the Per and Chl LHC is then passed on to Photosystem II (PS-II) to drive photosynthesis.

Excess light can lead to photoinhibition and photodamage in the PS-II of Symbiodiniaceae (Widiastuti et al., 2015). Per may reduce the photodamage caused by reactive oxygen species (ROS) when there is an excess in light absorption via non-photochemical quenching (NPQ) (Büchel, 2020; Slavov et al., 2016). This occurs when Per reduces photo-oxidizing singlet oxygen and chlorophyll triplet excitations by transferring excitation from the Chl onto the Per triplet state, thereby efficiently protecting Chl against photo-oxidation (Büchel, 2020; Damjanović et al., 2000).

Additionally, Slavov et al. (2016) found that in *Cladocodium* cells, NPQ converts excess amounts of energy into heat at the expense of fluorescence by shifting the excess excitation energy onto the more stable, Photosystem I (PS-I) (Slavov et al., 2016). However, long term exposure and increases in light stress may overwhelm these mechanisms, damaging the Symbiodiniaceae photosystem (Berg et al., 2021).

1.4.2 Xanthophylls, Diatoxanthin, and β -carotene

Xanthophylls and β -carotene are a class of pigments commonly found in plants and algae that are a subgrouping of carotenoids. Due to this classification, the protective mechanism of NPQ seen in peridinin is very similar to that of xanthophylls and β -carotene in seeking to avoid excess light

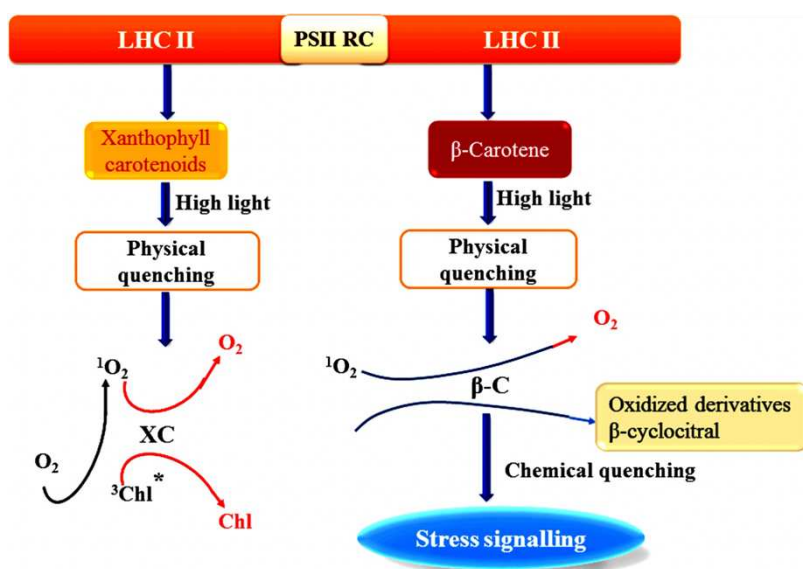


Figure 2: Xanthophyll, carotenoid, and β -carotene pathway in the PS-II, illustrating quenching and subsequent stress signaling (Diagram taken from Swapnil et al., 2021).

absorption. In xanthophylls, the photoprotective mechanism occurs in the LHC of the PS-II through a process called the xanthophyll cycle (XC) (Lavaud and Goss, 2014), while β -carotene is mainly found within the reaction center of the PS-II (Siefermann-Harms et al., 1978). The XC dissipates energy within light harvesting antenna, which reduces the amount of ROS. Additionally, if ROS are present within the reaction center, bioactive compounds derived from β -carotene form, creating stress signals that activate a plant's cellular defense system (Shumbe et al., 2014; Ramel et al., 2012) (Figure 2). In addition to processes brought about by xanthophylls and β -carotene, complex antioxidant activation networks in mitochondria and chloroplast are also upregulated in

order to combat ROS buildup (Foyer and Noctor, 2003), and have been found in terrestrial plants, microalgae, and in diatoms (Janknegt et al., 2009; Häubner et al., 2014; Sharma et al., 2012). These antioxidant activation networks have been found to work in tandem with the XC, as the production of antioxidants co-occurs with the XC (Smerilli et al., 2017). Additionally, XCs in diatoms have been found to de-epoxidize diadinoxanthin (Dd), a fluorescent pigment similar to that of Fx, Per, and β -carotene. Once Dd is de-epoxidized, it forms diatoxanthin (Dt), which is a photoprotective and recognized antioxidant pigment (Goss and Lepetit, 2015).

1.4.3 Flavoproteins

Many functional biological responses are stimulated by light, with two predominant forms: photosynthetic pigments that absorb light energy for oxygenic photosynthesis, and photosensory receptors that regulate light responses via non-photosynthetic means (Yu et al., 2010). These responses can be specific to different types of light, such as blue or ultraviolet light (UV). UV/Blue light responses occur through a subset of photoreceptors called Cryptochromes (CRY) (Gressel, 1979). CRY photoreceptors are found in many organisms, including algae, insects, coral, terrestrial plants, fish, and mammals, (Small et al., 1995; Emery et al., 1998; Levy et al., 2007; Tamai et al., 2007; Koornneef et al., 1980; Van Gelder et al., 2003). These CRYs are a type of non-photosynthetic photoreceptor (Ahmad & Cashmore, 1993) - categorized as flavoproteins due to flavin's central role in its chromophore (Briggs and Huala, 1999) - and will be referred to as flavin-based fluorescent proteins (FbFPs) from here onwards (Mukherjee et al., 2013; Drepper et al., 2007).

FbFP photobiochemistry relies on the excitation of electrons within the flavin protein by photons, whereby photoreduction changes the state of the CRY photoreceptor when exposed to blue light (Yu et al., 2010; Shalitin et al., 2002). This photoexcited CRY is then thought to become phosphorylated, adopt an open conformation, and interact with a signal partner protein (Yu, et al.,

2010; Liu et al., 2010). Through this process, FbFPs can moderate a myriad of functions in plants, such as gene expression, stress regulation, photomorphogenesis, phytochrome development, stomata activation, circadian rhythms, seedling de-etiolation, and flowering times (Nemhauser and Chory, 2002; D'Amico-Damião et al. 2018; Wang and Deng, 2002; McClung et al., 2002; Somers et al., 1998; Yu et al., 2010; Mao et al., 2005; El-Assal et al., 2001 & 2003; Kendrick & Kronenserg, 1994). Within corals, Levy et al. (2007) found that FbFPs were expressed within *Acropora millepora*, regulating their spawning times by sensing daylight and moonlight and contributing to mass spawning events (Harrison et al., 1984; Babcock et al., 1986). Additionally, FbFPs have been found to mediate the repair of DNA damaged by high levels of UV radiation (Sancar, 1994; Pokorny et al., 2008; Huang et al., 2006), as well as aid in the accumulation of antioxidants (Deng et al., 2014; Perumal et al., 2005; Taheri & Tarighi, 2010). However, our understanding of FbFPs is poorly understood within the context of Symbiodiniaceae. Regardless of the specific mechanisms, FbFPs, as well as peridinin, chlorophyll *a/c2*, xanthophylls, and β -carotene, have been linked to photoprotective mechanisms, and thereby, may serve as a proxy for coral health. As such, using the autofluorescent properties of these pigments provides insight into the state of photosystems and stress of Symbiodiniaceae, and if used in conjunction with our understanding of key differences found between *Acropora pulchra*, *Pocillopora damicornis*, and *Pavona decussata*, may unlock what is driving community composition shifts on Guam's reef flats.

1.5 Key Ecosystem Engineers on Guam's Reef Flats

1.5.1 *Acropora pulchra*

Guam's reef flats are characterized as expansive and shallow. These flats exhibit distinct zonation due to environmental pressures dependent on the distance from the reef crest/wave break,

tidal flux, currents, and flushing regimes, creating diverse coral communities (Raymundo et al., 2019). Of these coral communities, the most dominant genera are *Acropora*, *Pocillopora*, *Pavona*, and *Porites*. Two main types of reef flat communities are found on Guam: reef flats dominated by *Acropora* that appear to shift towards *Pavona*, and those dominated by *Porites*. In this project we focused only on the first type of reef flat community due to the observed community composition shifts between *Acropora pulchra*, *Pocillopora damicornis*, and *Pavona decussata*. *Acropora pulchra* (family Acroporidae) is found throughout the western Pacific and in the Indian ocean, including Guam and other western Pacific islands, Australia, Japan, the East China Sea, The Gulf of Aden, and along the equatorial areas of Eastern Africa and Madagascar (IUCN, 2008). *Acropora pulchra* is characterized by its staghorn shaped branches that contain tubular and radial axial corallites and indistinguishably sized thickets. The tubular corallites are much longer than the radial corallites, making them easily recognizable, while the radial corallites come in two sizes with one extending farther than the other form. Their branches can vary in coloration - from dark brown to a lighter brown-yellow color (Fenner, 2021). Within Guam, most *Acropora pulchra* populations reside on wide, shallow reef flats (Raymundo et al., 2022), with variation in coral morphology dependent on a colony's distance from the reef crest due to waterflow dynamics and the depth of low tide. *Acropora* species are known for their rapid growth, which allows for fast recovery after stress events, but makes them highly susceptible to disturbances (Boyett et al. 2007; Herlan & Lirman 2008). Rapid growth in staghorn *Acropora* is often associated with a "competitive" life history strategy, characterized by the ability to successfully compete for limited space through their efficient resource use and thus dominate a reef community by forming extensive thickets (Darling et al., 2012; Grime 1977; Grime & Pierce, 2012). *Acropora* are hermaphroditic spawners, though on Guam, staghorn species do not spawn at the same time as other congeners (Harrison et al., 1984; Hayashibara et al., 1997; Raymundo et al., *pers. comm*).

Acropora pulchra is also an important ecosystem engineer, creating large, complex habitats for various species and acting as a wave energy dissipator due to its three-dimensional thicket structure (Johnson et al, 2011; Kuffner & Toth, 2016).

1.5.2 *Pocillopora damicornis*

Pocillopora damicornis (family Pocilloporidae) has a wide distributional range, extending across tropical and subtropical parts of the Indian and Pacific oceans – specifically, Eastern Africa, the Red Sea, Southeast Asia, Japan, Australia, Hawaii, and the western coast of Central America (IUCN, 2014). *Pocillopora damicornis* are small, finely branching bushy corals, growing up to 30 cm in diameter. with verrucae bumps around 2-3 mm diameters wide and tall. Their corallites are characterized by small, 1mm in diameter, and are scattered across branches and in between the verrucae (Fenner, 2021). *Pocillopora damicornis* is recorded as having both brooding and spawning reproductive strategies (Schmidt-Roach et al., 2013; Ward, 1992), and coloration can range from purple, brown, to pale-brown. *Pocillopora damicornis* can have slight morphological differences, with stubby, compact, bush-like morphology in areas with higher wave action and water flow and more branched colonies in areas with calmer water flow farther from the reef crest (Veron, 1986). However, this high variability may be a result of unresolved species complexes. Its genus, *Pocillopora*, mostly follows a life history strategy described as a “weedy,” r-strategist, colonizing recently disturbed areas and exhibiting a short life span and high fecundity (Darling et al., 2012; Grime 1977; Grime & Pierce 2012). However, within Guam, this weedy colonization strategy does not seem to persist long term; observations detail quick settlement and growth that is subsequently followed by whole colony mortality soon after.

1.5.3 *Pavona decussata*

Pavona decussata (family Agariciidae) is native to western and central Indo-Pacific regions, extending along Eastern Africa, the Red Sea, the East China Sea, the Philippines, Japan,

Papua New Guinea, and Eastern Australia (IUCN, 2014). *Pavona decussata* forms vertical plates ranging from 1 cm to 10 cm tall, with an encrusting base. The corallites are usually small, ranging from 2-3 mm in size, and tentacles often extend during the day (Fenner, 2021), giving the coral a fuzzy appearance. *Pavona decussata* is a broadcast spawner (Mezaki et al., 2014; Okubo et al., 2014). Colony morphology is highly variable, with field observations detailing different morphotypes fusing together. *Pavona decussata*'s coloration usually ranges from brown-orange to yellow, and colonies are almost exclusively found on Guam's reef flats growing on *Acropora pulchra* rubble and skeletons, along with other dead coral species. The *Pavona* genus follows a mixed "generalist" and "stress tolerant" life history strategy (Darling et al., 2012); traits that both do well in habitats with low competition and allow for survival of stress events (Yu et al., 2020). Similar to *Pocillopora damicornis*, field observations have found that *Pavona decussata* replaces *Acropora pulchra* beds after stress events when *Acropora pulchra* is unable to recover.

1.6 Coral Species Replacement

Acropora corals have dominated tropical reef ecosystems for roughly 250,000 years, surviving fluctuations in various temperature and sea levels (Jackson, 1992; Greenstein et al., 1998; Pandolfi et al., 2006). However, *Acropora* populations are now collapsing, with species replacements and community composition shifts from Acroporidae to Agariciidae and Pocilloporidae occurring worldwide (Roff et al., 2013; McClanahan, 2004, 2008; Cramer et al., 2012). On the Great Barrier Reef, sediment cores have shown an abrupt transition from *Acropora* assemblages to almost exclusively *Pavona* beds on inshore reefs, coinciding with stress events experienced on inshore islands between 1928 and 1944 (Roff et al., 2013). Additionally, over the last 30 years, the percentage cover of *Pavona* and *Pocillopora* has increased on Kenyan reefs, while fast-growing, branching Acroporidae genus' such as *Acropora* and *Montipora* have

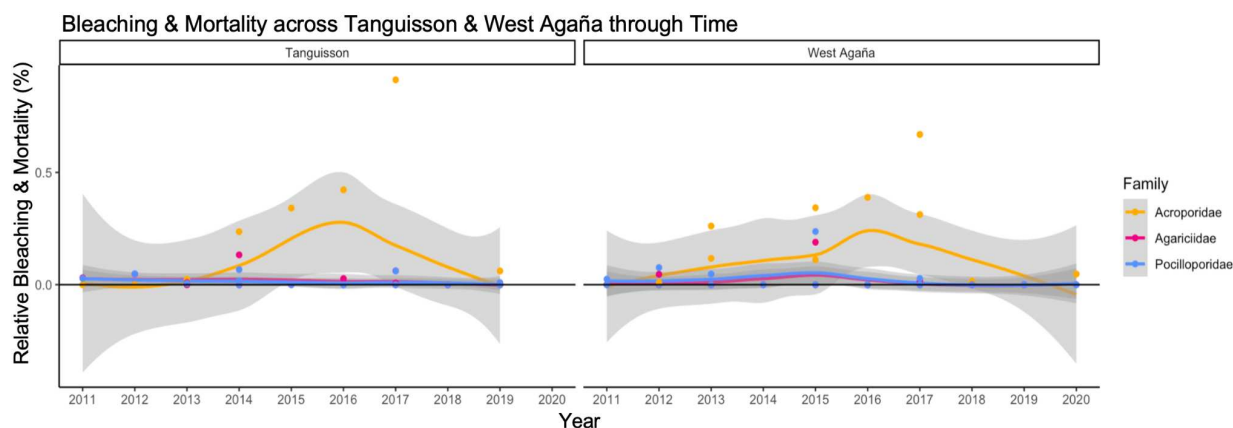


Figure 3: 2011-2020 mean percent bleaching and mortality for three coral families. Acroporidae, Agariciidae and Pocilloporidae abundance values correlated with the mean percent (%) affected in terms of bleaching and mortality across West Agaña and Tanguisson from 2011-2020 (Data taken from Raymundo et al., *in prep*).

displayed little to no recovery after stress events (McClanahan, 2008). Furthermore, during a 1998 heat wave in Kenya, encrusting and sub-massive *Pavona* species (*Pavona varians*, *Pavona decussata*, and *Pavona venosa*) were unaffected (McClanahan, 2004), potentially paving the way for the community composition shifts that have followed since. Replacements of Acroporidae populations by certain Agariciid species is also occurring in the Caribbean. This replacement predates any current diseases present in the region and mass bleaching events, indicating that these may have been long-term trends that are now being accelerated by global stressors (Cramer et al., 2012; Aronson & Precht; 1997).

On Guam, evidence of high bleaching and mortality of Acroporidae contrasts with that of Agariciidae, and Pocilloporidae (Figure 3). This difference in resilience likely contributed to community composition shifts from *Acropora pulchra*-dominated reef flats to *Pavona decussata*- and *Pocillopora damicornis*-dominated reef flats, and has been observed with the recruitment of multiple species such as: *Pavona decussata*, *Pocillopora damicornis*, *Porites cylindrica*, *Porites divaricata*, *Psammocora contigua*, and *Leptastrea purpurea* (Raymundo et al., 2019). However, our knowledge of changes in abundances of *A. pulchra*, *Pocillopora damicornis*, and *Pavona decussata* species is limited. Therefore, because an ecosystem drives much of an organism's

functional abilities and coral species interact in highly complex ecological spaces, understanding species interactions between *Acropora pulchra*, *Pocillopora damicornis*, and *Pavona decussata* across the family, genus, and species level is integral. As such, understanding how anthropogenic disturbances have changed community compositions within reefs on Guam and throughout the world is needed in order to understand potential future community composition shifts.

1.7 Abiotic Factors that Shape Guam's Reef Flats

1.7.1 Vertical Tectonic Motion

Due to Guam's location on the Mariana Convergent Plate Region (MCPR) and its tropical location, the geologic history of the island has been shaped by volcanic, tectonic, and coral processes beginning with the emergence of the island in the Eocene some 30-50 million years ago. However, these processes were not uniform, with uneven emergence and submergence events occurring frequently and on different parts of the island due to MCPR faulting processes (Randall & Eldredge, 1977; Randall, 1979). These uneven events have contributed to multiple limestone terraces that can be seen on Guam's northern cliffs (Randall & Eldredge, 1977; Taboroši et al., 2004), of which one is the remnants of Holocene reefs that had formed around 4,000 years B.P. (before present) (Kayanne et al., 1993; Siegrist & Randall, 1992). Furthermore, these emergence and submergence events have been documented in other areas of the Pacific that are on or near convergent plates, such as in the Torres group of the Vanuatu arc. Here, the last hundred thousand years have been marked by intense uplift events, averaging at a rate of 0.7 - 0.9 mm/yr (Taylor et al., 1985). As such, due to these emergence and submergence events, Guam's reef flat structure has changed repeatedly over geologic timescales and have likely caused Guam's reef flats to

become shallower and deeper over time, with present-day reef flats being extremely shallow, at times exposed during low tides.

1.7.2 Tidal Exposure

Guam's reef flats are mostly found on the leeward side of the island and are characterized as expansive and shallow. They range in depth from <0.1m to 2m, with the reef crest being 0.1m to 1m in depth and the nearshore reef having an average depth of 1m to 2m. Due to this difference in depth, the reef crest is often exposed during low tide events. However, Guam's tidal events are exacerbated during spring tides, which exposes much of the reef flat and is a prominent limiting factor for coral growth (Heron et al., 2020). Additionally, when ENSO is combined with usual low tide events, (leading to extreme low tides and aerial exposure), high levels of mortality have occurred (Loya, 1976; Anthony & Kerswell, 2007; Heron et al., 2020). On Guam, Heron et al. (2020) categorized 50% of Guam's shallow reef flats as having moderate to high vulnerability to ENSO-related extreme low tide events. These ENSO-related extreme low tide events caused significant mortality for reef flat corals, especially among *Acropora* species (Heron et al., 2020).

1.7.3 Water Flow Dynamics

Coral reef communities vary with wave exposure, and reef zone (reef flat, reef crest, reef slope). This pattern is driven by abiotic factors such as water flow dynamics, light penetration, and temperature (Done, 1982; Hughes et al., 2012; Graham et al., 2006). However, differences within coral reef communities can also exist within a zone (Raymundo et al., 2019). This interspecific difference is important when considering stress events, such as projected increases in SSTs which will increase the frequency of coral bleaching events (Hoegh-Guldberg, 1999, 2017; Hughes et al., 2017b) and affect corals worldwide and on Guam. Furthermore, coral bleaching and mortality is not uniform across spatial scales, with certain zones on a reef flat being more susceptible or

resilient to bleaching and mortality (Raymundo et al., 2017, 2022). This variation within a reef flat zone suggests that water flow dynamics play a large role on a reef scale (Anthony & Kerswell, 2007; Johansen, 2014, Fifer et al., 2021) by reducing SSTs around a coral (Bayraktarov et al., 2013; Fujimura & Riegl, 2017; Smith & Birkeland, 2007) and increasing recovery in bleached corals (Nakamura et al., 2003). Differential patterns in reef flat bleaching and mortality were exemplified during the 2013-2017 bleaching event, where coral populations - in particular, Acroporids - on Guam showed significantly more bleaching and mortality nearshore, whereas populations closer to the reef crest showed significantly less bleaching and mortality (Raymundo et al., 2017). Additionally, water flow dynamics on Guam fluctuate depending on the season, with winter months experiencing large swell events that increase water flow and summer months experiencing calmer, reduced water flow dynamics. As such, due to Guam's well-documented history of emergence, extreme tidal exposures, and differing water flow dynamics, Guam's current reefs may be experiencing conditions that may also be driving community composition towards certain species, and an increased understanding of coral responses to changing environmental parameters will be imperative to the success of management, restoration, and conservation projects on Guam.

1.8 Research Questions

Species replacements away from *Acropora pulchra* towards *Pocillopora damicornis* and *Pavona decussata* have been observed over the last decade, yet the mechanisms driving the decline of *A. pulchra*'s and increase in *P. damicornis* and *P. decussata* have yet to be understood. As such, the objectives of this proposed research were to: **1)** examine how physiological differences between these three corals may be driving coral community composition shifts away from

Acropora pulchra towards *Pavona decussata* and *Pocillopora damicornis* on Guam's reef flats. **2)** Quantify *Acropora pulchra*, *Pocillopora damicornis*, and *Pavona decussata* community cover and abundances across temporal and spatial scales. **3)** Characterize Symbiodiniaceae communities associated with *Acropora pulchra*, *Pocillopora damicornis*, and *Pavona decussata*. **4)** Infer how *Acropora pulchra*, *Pocillopora damicornis*, and *Pavona decussata*'s Symbiodiniaceae communities may differ in their functions and thus contribute to the decline of *Acropora pulchra*.

1.8.1 Null and Alternative Hypotheses

H₀₁: Reef community compositions will not differ across temporal and spatial scales.

H_{A1}: Reef community compositions will differ across temporal and spatial scales.

H₀₂: Coral-associated Symbiodiniaceae assemblages will not differ across species, and temporal, and spatial scales.

H_{A2}: Coral-associated Symbiodiniaceae assemblages will differ across species, and temporal, and spatial scales.

H₀₃: Coral-associated Symbiodiniaceae functionality will not differ across temporal, spatial, and species scales.

H_{A3}: *Acropora pulchra* Symbiodiniaceae functionality will differ across temporal and spatial scales, whereas *Pocillopora damicornis* and *Pavona decussata* Symbiodiniaceae functionality will remain consistent.

1.9 MATERIALS AND METHODS

1.9.1 Study Location

Coral samples collection and ecological monitoring were completed at two reef flats located on the island of Guam: West Agaña (N 13.47993° E 144.74278°) and Tanguisson (N 13.54874° E 144.81026°) (Figure 4). These two sites represent different environmental conditions, water flow dynamics, and coral biodiversity (Raymundo et al., 2017). West Agaña is characterized by a wide, shallow reef flat containing a combination of pavement (non-living substrate), sand patches, and patchy coral communities and encompasses the Agaña Wastewater Treatment Plant

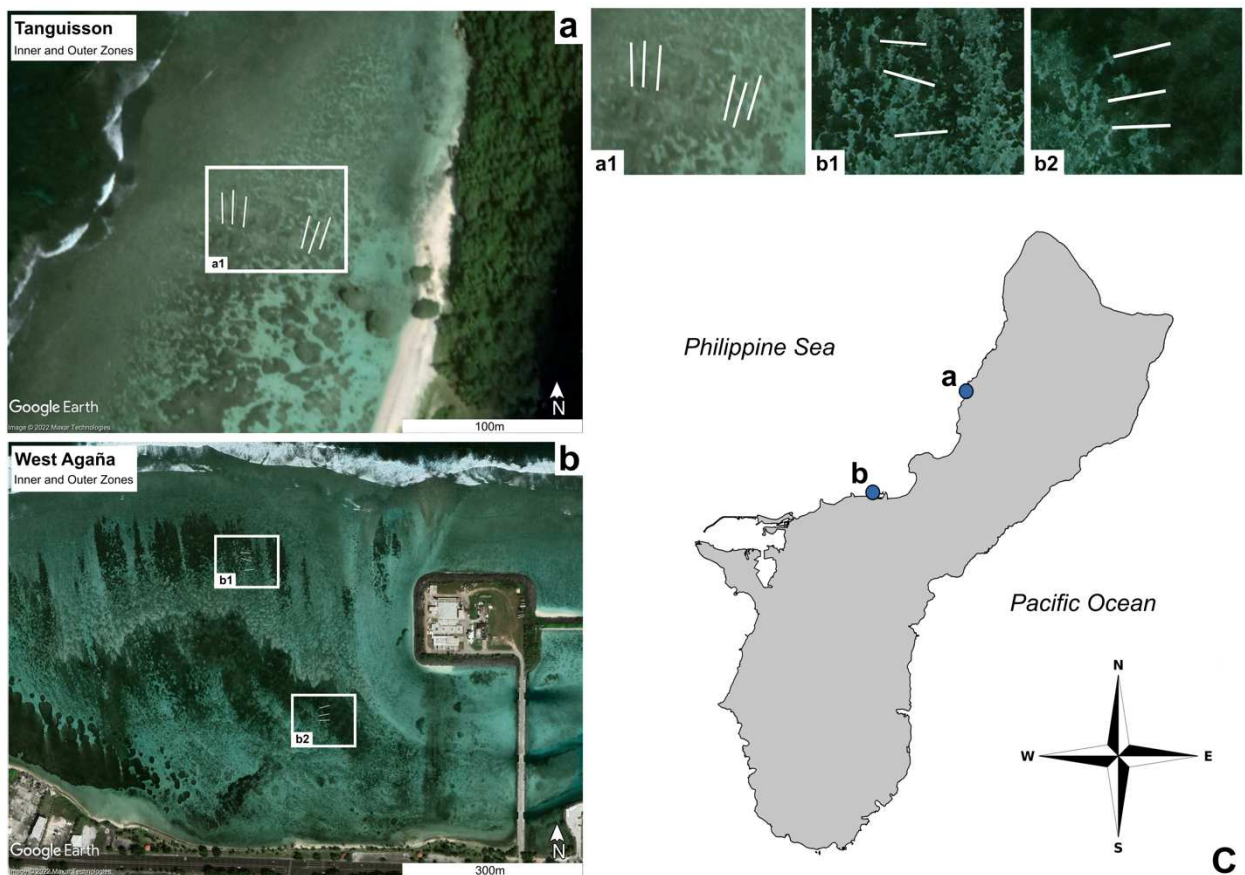


Figure 4: Tanguisson (A) and West Agaña (B) field site with six 15m fixed transect tapes rolled out parallel to shore for inner and outer zones (A1, B1, B2).

within its northwestern boundary, and is nearshore to a sewage outfall pipe (Raymundo et al., 2022). Near the reef crest, staghorn coral *Acropora pulchra* dominates, *Porites lobata* is common, and various coral species make up the rest of the assemblages at low levels, while *Pavona decussata* and *Pocillopora damicornis* colonies are scarce. Within the inner zone, however,

Pavona decussata dominates, with lower abundance of *Acropora pulchra* thickets. West Agaña also has evidence of high species replacement of staghorn thickets with recruits of *Pavona decussata* and *Pocillopora damicornis* establishing themselves onto dead *Acropora pulchra* skeletons (Raymundo, et al., 2019) (Figure 3A). This site also experiences differences in water flow and turbidity dependent on proximity to the reef crest: higher water flow and lower turbidity near the reef crest and lower water flow and higher turbidity nearshore (Raymundo et al., 2017). These differences resulted in higher past bleaching and mortality related events for nearshore *Acropora pulchra* colonies (Raymundo et al., 2019; Fifer et al., 2021).

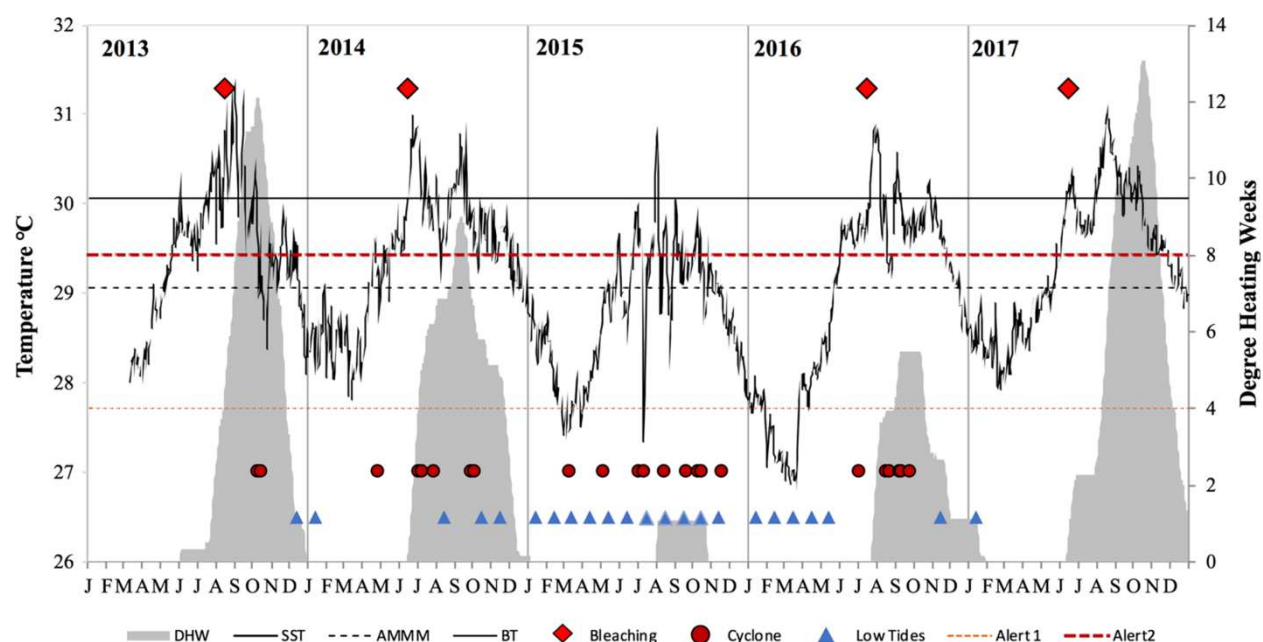


Figure 5: 2013–2017 time series of running 7-d mean sea surface temperature (SST) from the NOAA CRW virtual station for Guam plotted against annual maximum monthly mean SST (AMMM), bleaching threshold (BT), and degree heating weeks (DHW) for 2013–2017 (Diagram taken from Raymundo et al., 2019). Coral samples were collected at four different timepoints.

Tanguisson is characterized by a narrow, shallow reef flat that is exposed to high water flow and extreme low tidal events. Before the 2013 bleaching event, this site was dominated by extensive *Acropora pulchra* thickets that have been reduced by 80% after repeated mortality events (Raymundo et al., 2017; Raymundo et al., 2019). Currently, the outer zone is characterized by scattered staghorn thickets, wave resilient coral species, and low abundances of *Pavona decussata*

and *Pocillopora damicornis*, while the inner zone is characterized by higher abundances of *Pavona decussata* and a small number of *Acropora pulchra* thickets. It is interesting to note that *Pocillopora damicornis* is rare in Tanguisson with the exception of a few colonies in the inner zone of both sites. Unlike West Agaña, this site seems to experience very little differences in water flow and turbidity dependent on proximity to the reef crest due to its narrow reef flat.

1.9.2 Ecological & Environmental Monitoring

At each of the two sites (Tanguisson and West Agaña), six 15m replicate transects were laid 5m apart: three at the inner zone and three at the outer zone, parallel to the reef margin (Figure 3,4). Transect start and endpoints were marked by GPS, and each transect was monitored across

two time points: Timepoint

1: February 2022 (pre-warming period) and

Timepoint 3: August 2022 (peak warming period)

(Figure 5,6). Along the transects, 1m² quadrats were laid every other meter to quantify immediate live

percent coral cover. In order to make sure that the

quadrats covered the same area across time points, we positioned nails every 5 meters to reduce the margin of error in quadrat monitoring. These surveys provided quantitative estimates of benthic components, such as coral and non-coral percent coverage, over spatial (Tanguisson Inner/Outer and West Agaña Inner/Outer) and temporal (T1 - February, T3 - August) scales.

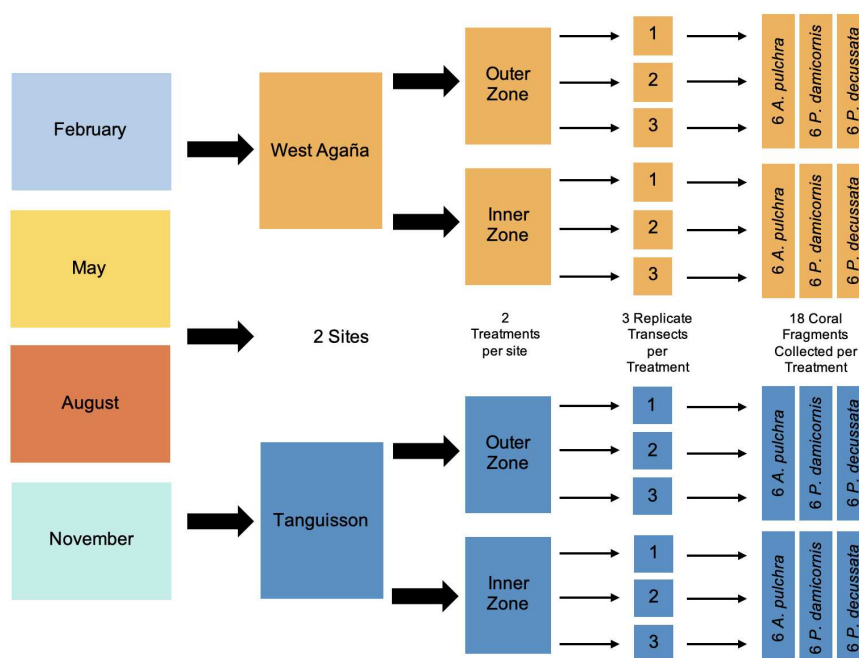


Figure 6: Experimental design; illustrating two sites (Tanguisson and West Agaña), each with two treatments (inner and outer zone) and three transects per treatment zone. Within each transect, two *A. pulchra*, *P. damicornis*, and *P. decussata* were tagged and sampled across four timepoints.

To quantify water temperatures, four Onset HOBO temperature loggers (Onset, Bourne, MA) were deployed at each site (two in the inner zone, two in the outer zone) and collected temperature measurements in 15-minute increments. Two TCM-4 Shallow water Tilt Current Meters (Lowell Instruments, East Falmouth, MA) were deployed between the months of December 2022 and February 2023 at each site (one inner, one outer) to determine water flow dynamics at each site and zone. These data were then correlated with ecological monitoring data to help distinguish inferences between water flow, temperature, and mortality. Additionally, publicly available precipitation data was obtained to identify yearly changes in rainfall (Menne et al., 2012).

1.9.3 Field Collection

288 individual coral colonies of *Acropora pulchra*, *Pocillopora damicornis*, and *Pavona decussata* were tagged and sampled (N = 72/timepoint) across both sites at each timepoint along the same six 15m fixed transects used for our ecological monitoring. Target colonies were divided equally into inner and outer zones (Figure 5), with sampling of these tagged coral colonies done at four different timepoints. Timepoint 1: February 2022 (pre-warming period), to collect baseline measurements. Timepoint 2: May (transitional pre-warming period), to collect transitional measurements between baseline and peak periods. Timepoint 3: August 2022 (peak warming period), to collect peak period. Timepoint 4: November 2022 (transitional post-warming period), to collect potential recovery dynamics within transitional measurements after the peak period. Corals were sampled using a small hammer and chisel and stored in Whirl-pak® sampling bags (Whirl-Pak, Madison, WI), drained of any residual water, and then flash-frozen using liquid nitrogen. Enough coral fragments were collected in order to have sufficient amounts for DNA extractions and cytometry. These samples were then organized by timepoint and species and stored in a -80°C freezer to maintain genetic and cellular integrity. Additionally, each coral colony was

photographed during T1 (February) sampling and then again during T3 (August) sampling to monitor for environmental responses.

1.9.4 Symbiodiniaceae Biodiversity

In order to identify Symbiodiniaceae communities within *Acropora pulchra*, *Pocillopora damicornis*, and *Pavona decussata*, flash-frozen DNA from sampled coral tissues were extracted using the Qiagen DNeasy® PowerSoil Pro Kit® with a Qiacube extraction robot (Qiagen, Hilden, Germany). The Internal Transcribed Spacer 2 (ITS2) region was amplified using 30ng of DNA extract by PCR using the following profile: 26x(95°C for 40 sec, 59°C for 2 min, 72°C for 1 min), 72°C for 7 min using SYM_VAR_5.8S2 and SYM_VAR_REV primers (Hume et al., 2018). These were then amplified using the following profile: 5x(95°C for 40 sec, 59°C for 2 min, 72°C for 1 min), 72°C for 7 min and then barcoded with an Illumina index primer that had been amplified with the following profile: 5°C for 5 min, 12x(95°C for 40 sec, 63°C for 2 min, 72°C for 1 min). The barcoded samples were then placed together in a 96-well plate, run on a 2% agarose gel using SYBR green dye, cut to the desired size, and soaked in MiliQ water at 4°C until the following day. The samples were then combined with P5 and P7 sequence adapters to make sure that the PCR is viable and then purified using a GeneJet PCR purification kit (ThermoFisher Scientific, Rockford, IL, USA) after the ITS2 amplification and pooling process. These ITS2 amplicons were then multiplexed and sequenced on a NovaSeq 6000 (250bp Paired ends) (Illumina, San Diego, CA, USA). Once our products were amplified, sequences were demultiplexed to remove primers and barcodes and submitted to SymPortal for Symbiodiniaceae identification via differentiation of inter and intragenomic sources of ITS2 sequence variance (Hume et al., 2019) to determine Symbiodiniaceae densities within *Acropora pulchra*, *Pocillopora damicornis*, and *Pavona decussata* between February and August.

1.9.5 Symbiodiniaceae Density & Autofluorescence

Using a modified version of the cytometry method described in Krediet et al. (2015) and Anthony et al. (2022), coral samples were airbrushed using filtered seawater (FSW) to extract tissue from the skeleton and homogenized with a 10 mL latex-free syringe, ensuring that this was

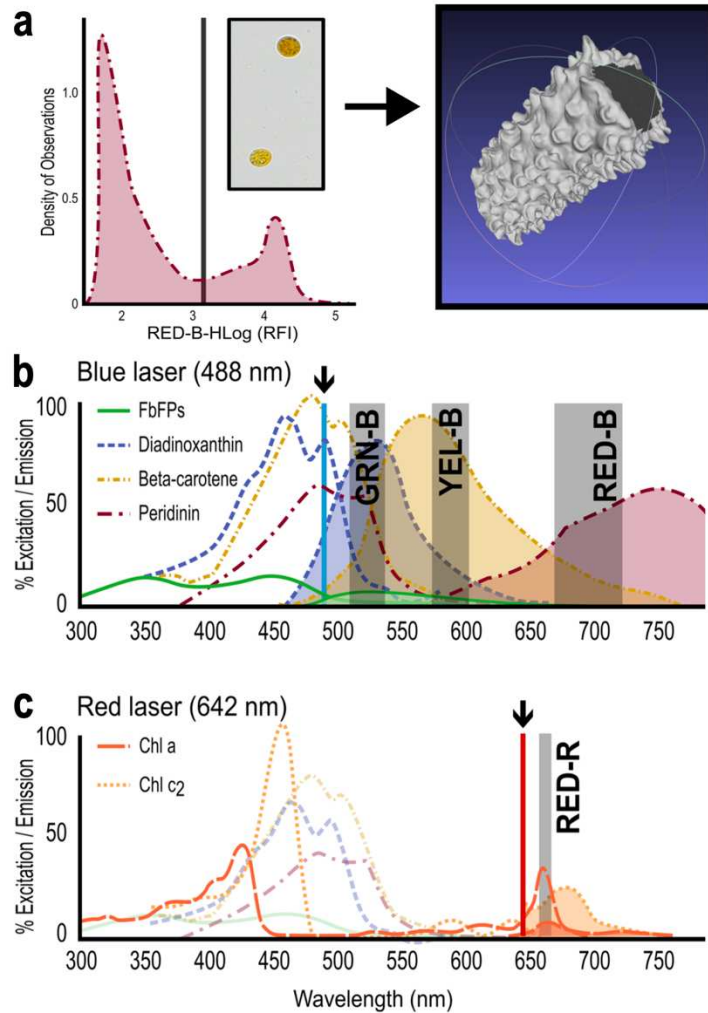


Figure 7: **a).** Symbiodiniaceae forward + side scatter to calculate cell densities via Guava easyCyte Flow Cytometer wavelength lasers and 3D mesh model used to normalize Symbiodiniaceae cell counts. **b).** (BLUE BAND): Per and antioxidant associated pigment excitation at 488 nm via the blue laser. Green, Yellow, and Red filters used to determine specific pigments **c).** (RED BAND): Chl *a/c*₂ excitation at 642 nm via the red laser and red filtration. (Diagram taken from Anthony et al., 2022).

accomplished in the dark and on ice to maintain pigment levels and reduce sample degradation. A 1 mL of homogenized tissue slurry was transferred into a 1.5 mL tube, with the rest of the slurry being measured with a graduated cylinder. The 1 mL slurry was then homogenized using a MiniBeadBeater Plus for four seconds to remove mucus from the Symbiodiniaceae, and centrifuged at 5000 rpm for four minutes at -10°C. Once centrifuged, the supernatant was discarded and a second resuspension of the pellet using 1 mL of FSW was performed. A second set of 4-second homogenization in the MiniBeadBeater Plus and a 5000 rpm centrifugation for three minutes at -10°C was done to clean the pellet further. The second supernatant was then discarded, and the remaining pellet was resuspended in 1 mL of sodium dodecyl sulfate (SDS) solution (.08% w/v SDS, 7/8 deionized water (DI), 1/8 FSW) and loaded

accomplished in the dark and on ice to maintain pigment levels and reduce sample degradation. A 1 mL of homogenized tissue slurry was transferred into a 1.5 mL tube, with the rest of the slurry being measured with a graduated cylinder. The 1 mL slurry was then homogenized using a MiniBeadBeater Plus for four seconds to remove mucus from the Symbiodiniaceae, and centrifuged at 5000 rpm for four minutes at -10°C. Once centrifuged, the supernatant was discarded and a second resuspension of the pellet using 1 mL of FSW was performed. A second set of 4-second homogenization in the MiniBeadBeater Plus and a 5000 rpm

into a 96-well microwell plates as part of a tenfold 50:50 DI:FSW dilution. These replicates were then processed by a Luminex Guava easyCyte 6HT-2L flow cytometer (Luminex Corporation, Austin, TX). To collect Symbiodiniaceae counts, red fluorescent emissions (695 ± 50 nm) from blue light excitation (488 nm laser) and forward and side scatter (Krediet et al. 2015) was used (Figure 7). Cell counts (cells/mL) were multiplied by ten to account for the dilution done earlier, which gave us relative cellular densities. In order to obtain actual cellular densities, coral skeletons were coated in SKD-S2 Aerosol (Magnaflux, Glenview, IL) to reduce light refraction and then 3D-scanned with a .010nm point cloud (D3D-s, Vyshneve, Ukraine). These 3D models were then imported into MeshLab v2020.04 (Cignoni et al. 2008) to create a surface mesh using a screened Poisson surface reconstruction. Surface area of the model was calculated using Blender, making sure to exclude areas that did not include coral tissue (Figure 7). The relative cellular densities were then normalized using the coral skeleton's surface area. Relative fluorescent intensity (RFI) values were determined via three profiles (Figure 7) (Anthony et al., 2022): a red emission (695/50 nm) off blue (488 nm) excitation laser (RED-B) for the target pigment peridinin (Bujak et al., 2009), a red emission (661/15 nm) off red (642 nm) excitation laser (RED-R) for Chl *a/c2* (Niedzwiedzki et al., 2014), and a green emission (525/30nm) off blue (488 nm) excitation laser (GRN-B) for antioxidant associated fluorescent proteins such as FbFPs , xanthophylls, and β -carotene (Mukherjee et al., 2013; Kagatani et al., 2022; Lee et al., 2019; Van Riel et al., 1983). Once completed, RFIs were attached to the coral sample it was associated with, providing potential ecophysiological functions of Symbiodiniaceae populations in each target species, which were used to infer key differences among *Acropora pulchra*, *Pocillopora damicornis*, and *Pavona decussata*.

2.0 Statistical Analysis

Due to violations in normality, environmental data such as temperature and precipitation were compared using a Kruskal-Wallis nonparametric test. Temperature data interactions included time (February, May, August, November) site (Tanguisson, West Agaña), and zone (Inner, Outer), while precipitation was only compared across time (February, May, August, November) since there was no site-specific data. Temperature and precipitation data from each month was spliced to only include months where sample collection was done to reduce unnecessary noise from months without sample collection. Water flow dynamics were compared using analysis of variance (ANOVA) to highlight potential differences across time (December, January, February), site (Tanguisson, West Agaña), and zone (Inner, Outer). To quantify differences in percent cover and abundance, Kruskal Wallis nonparametric tests were used to identify differences across time, site, zone, and benthic component.

To compare differences in Symbiodiniaceae community compositions, time (February, August), site (Tanguisson, West Agaña), zone, (Inner, Outer), and species (*Acropora pulchra*, *Pavona decussata*, *Pocillopora damicornis*) were analyzed from post-MET normalized Symportal ITS2 sequence abundance types. These comparisons included multivariate homogeneity of dispersion (PERMDISP), pairwise permutation tests, and permutational multivariate analysis of variance (PERMANOVA) tests via *Vegan* v2.5-7 (Oksanen et al., 2019) and pairwise Adonis v0.4 (Martinez Arbizu, 2017) packages. To determine differing contributing factors within Symbiodiniaceae physiology, Repeated Measures, Multivariate Analysis of Variance (RM-MANOVA) were conducted to evaluate peridinin, chlorophyll, and antioxidant associated fluorescent pigment signatures, as well as cellular densities using Time*Species*Site*Zone. All statistical analyses were completed with R v4.2.2 statistical environment (R Core Team 2022) in

RStudio v2022.12.0+353 (RStudio Team 2022). Figures were generated using *ggplot2* v3.4.0 (Wickham 2016).

2.1 RESULTS

2.1.1 Environmental Factors

Sea surface temperatures (SSTs) at both Tanguisson and West Agaña showed increases from February to June 2022, ramping up from 28°C to 30°C. These site temperatures then fluctuated around 30-31°C from June until October 2022 before beginning to decrease below 30°C in November 2022 (Figure 8). We found significance in time ($\chi^2 = 238.45$, $p < .001$), but no significance when considering sites or zones. However, when looking at interaction effects, site and zone was significant ($\chi^2 = 9.817$, $p < .05$) indicating potential differences between each site and zone combination. Precipitation levels followed the seasonal wet/dry cycle on Guam, with the driest period occurring from January through May, and the wettest months steadily increasing in precipitation in June and peaking during September and October, after which the dry season began again (Figure 8a). Significant differences in precipitation were observed across time ($\chi^2 = 12.905$, $p < .005$). Water flow dynamics were found to have major differences across both temporal and spatial scales (Figure 9). We found that there was significance in time ($F = 63.659$, $p < .001$), site ($F = 77.096$, $p < .001$), and zone ($F = 104.023$, $p < .001$), with site and zone interactions having a significant effect ($F = 79.836$, $p < .001$). Site differences were characterized by Tanguisson having overall higher water flow, as well as higher peak flows than West Agaña. Zone differences were characterized by higher water flow in outer zones compared to that of inner zones (Figure 9).

2.1.2 Ecological Monitoring

Percent coral cover at both Tanguisson and West Agaña showed no significant differences across time or zone, with site ($\chi^2 = 9.738$, $p < .005$) and benthic component ($\chi^2 = 353.23$, $p < .001$)

differences being the only significant factors. To determine if non-living substrate and algal cover was significantly different than live coral cover, all coral species were combined as “Coral” and all non-living substrate and algae were aggregated as “Non-Coral.” Results illustrated that there were significant differences in Non-Coral and Coral cover ($\chi^2 = 202.3$, $p < .001$), but time was insignificant. Abundance data showed similar results, with significant differences in coral abundance between sites ($\chi^2 = 5.718$, $p < .05$) and benthic component ($\chi^2 = 607.51$, $p < .001$), but not time or zone.

2.1.3 Symbiodiniaceae Community Diversity

Beta diversity dispersion was significantly determined by species ($F = 561.48$, $p < .001$) and site zone ($F = 4.5251$, $p < .005$), but not site ($F = 3.3568$, $p > .05$) or zone ($F = 2.4086$, $p > .05$). Pairwise Adonis tests revealed that species explained the most variance (*A. pulchra* vs *P. damicornis*: $F = 59.227$, $R^2 = .3865$, $p < .001$; *A. pulchra* vs *P. decussata*: $F = 23.118$, $R^2 = .1974$, $p < .001$; *P. damicornis* vs *P. decussata*: $F = 92.028$, $R^2 = .4947$, $p < .001$) (Table 3). Site was significant (Tanguisson vs West Agaña: $F = 2.731$, $R^2 = .0189$, $p = .021$), with time (February vs August: $F = 1.726$, $R^2 = .0120$, $p = .1091$), and zone (Inner vs Outer: $F = 1.948$, $R^2 = .0135$, $p = .0748$) being nonsignificant (Table 3). Interestingly, only comparisons with Tanguisson Inner were found to be significant when looking at site and zone interactions (Tanguisson Inner vs Tanguisson Outer: $F = 2.957$, $R^2 = .0405$, $p = .0320$; Tanguisson Inner vs West Agaña Inner: $F = 4.256$, $R^2 = .0573$, $p = .008$; Tanguisson Inner vs West Agaña Outer: $F = 4.110$, $R^2 = .0554$, $p = .008$; Tanguisson Outer vs West Agaña Inner: $F = .8423$, $R^2 = .0119$, $p = .559$; Tanguisson Outer vs West Agaña Outer: $F = .7769$, $R^2 = .0109$, $p = .559$; West Agaña Inner vs West Agaña Outer: $F = 1.1664$, $R^2 = .01638$, $p = .4598$) (Table 3). Upon further investigation, it was found that *Acropora pulchra* colonies within Tanguisson Inner were outliers (*A. pulchra* Tanguisson Inner vs *A. pulchra* Tanguisson Outer: $F = 13.8379$, $R^2 = .3861$, $p < .001$); *A. pulchra* Tanguisson Inner vs *A. pulchra*

West Agaña Inner: $F = 18.3346$, $R^2 = .4547$, $p < .001$; *A. pulchra* Tanguisson Inner vs *A. pulchra*
 West Agaña Outer: $F = 19.6035$, $R^2 = .4712$, $p < .001$; *A. pulchra* Tanguisson Outer vs *A. pulchra*
 West Agaña Inner: $F = .9663$, $R^2 = .0421$, $p = .4318$; *A. pulchra* Tanguisson Outer vs *A. pulchra*
 West Agaña Outer: $F = 1.2024$, $R^2 = .0518$, $p = .4029$; *A. pulchra* West Agaña Inner vs *A. pulchra*
 West Agaña Outer: $F = .2767$, $R^2 = .0124$, $p = .7845$), with *P. damicornis* and *P. decussata* site and zone comparisons being insignificant (Table 4). Symbiodiniaceae communities within *Pocillopora damicornis* colonies displayed high levels of *Durusdinium* D1 regardless of site or zone, with *Durusdinium* D2d being the second most prevalent group (Figure 12). Within *Pavona decussata*, Symbiodiniaceae communities consisted primarily of *Cladocopium* C1 and *Cladocopium* C1c, showing little variance across site or zone (Figure 12). Within *Acropora pulchra*, *Cladocopium* C40 dominated in colonies found within West Agaña and Tanguisson outer, followed by small proportions of *Cladocopium* C3 and *Cladocopium* C40al. Tanguisson Inner colonies, however, displayed majority *Durusdinium* D1 and *Durusdinium* D4 symbiont types (Figure 12). This resulted in Symbiodiniaceae communities appearing to be varied across site and zone but were stable across spatial scales when excluding Tanguisson Inner *Acropora pulchra*.

2.1.4 Symbiodiniaceae Densities & Autofluorescence

Repeated Measures MANOVA identified that site and species were the strongest contributors to variation within cellular densities, peridinin, chlorophyll, and antioxidant associated RFIs (Table 1). Coral associated Symbiodiniaceae densities were regulated differently depending on time ($F = 2.905$, $p < .05$), site ($F = 78.841$, $p < .001$), and species ($F = 45.452$, $p < .001$), but not zone or site and zone, with Tanguisson corals harboring greater Symbiodiniaceae densities than West Agaña corals (Figure 13). Between species, pooled cell counts showed that *Pavona decussata* had the highest average density of Symbiodiniaceae (2.06×10^6 cells/cm²), followed by *Acropora pulchra* (1.75×10^6 cells/cm²) and *Pocillopora damicornis* (1.08×10^6

cells/cm²). Additionally, *Acropora pulchra* and *Pocillopora damicornis* associated Symbiodiniaceae densities from Tanguisson and West Agaña converged by November, whereas *Pavona decussata*'s Symbiodiniaceae densities stayed distinct across site (Figure 13). *Acropora pulchra*'s Symbiodiniaceae densities also demonstrated clear decreases in May and August from February levels, before increasing again in November, whereas *Pocillopora damicornis* and *Pavona decussata*'s Symbiodiniaceae densities increased in May and August before decreasing to February levels in November.

Peridinin associated RFI levels were significantly different across time ($F = 902.138$, $p < .001$), site ($F = 27.557$, $p < .001$), and species ($F = 266.210$, $p < .001$), with the interaction between site and zone also proving significant ($F = 26.331$, $p < .001$) (Table 1). Within chlorophyll associated RFI, every factor was significant: time ($F = 353.091$, $p < .001$), site ($F = 162.182$, $p < .001$), zone ($F = 41.502$, $p < .001$), and species ($F = 131.174$, $p < .001$), with time being the largest contributing factor (Table 1). Similar to Peridinin associated RFI, site and zone interactions were also significant ($F = 58.313$, $p < .001$) (Table 1). Pearson correlations tests on peridinin and chlorophyll autofluorescent linear models pooled between time, site, and species revealed a significant positive correlation ($r = 0.55$, $p < .001$), with slope and R^2 value lending additional strength (slope = .755, $p < .001$; $R^2 = .307$, $p < .001$) to this trend. Additionally, specific temporal, spatial, and species linear models indicated highly specific results (Appendix Table 1A), but due to limited statistical power, these models were not focused on, instead identifying larger temporal differences between species.

Antioxidant associated RFIs were significantly different across time ($F = 162.686$, $p < .001$), site ($F = 267.080$, $p < .001$), and species ($F = 225.430$, $p < .001$), with zone being the only insignificant factor (Table 1). Site was found to be the largest contributing factor, followed closely by species, and then time. Interactions between site and zone were also significant ($F = 26.430$, p

< .001). Comparisons between time, site, and species showed varied responses in antioxidant RFI levels to seasonal trends. West Agaña *Acropora pulchra* antioxidant associated RFIs stayed consistently high when compared to Tanguisson *A. pulchra*, but fell sharply by November (Figure 14). *Pocillopora damicornis* antioxidant associated RFIs showed significant variations between sites in February and November but converged in May and August as SSTs were at their highest. *Pavona decussata*, however, expressed consistently low antioxidant associated RFI when compared to *Acropora pulchra* and *Pocillopora damicornis*, and experienced no difference between sites. Although the severity of expression differed between species across time, all species experienced increased antioxidant associated RFIs as SSTs rose from February to August, followed by a decrease as SSTs fell in November.

2.2 DISCUSSION

2.2.1 Reef Community Stability

We found that although there were significant differences in community composition across benthic component and site between February and August, significant differences over temporal scales were not observed. This is likely due to the short nature of our ecological monitoring, which did not allow us to capture regenerative effects that could have illustrated species replacement from Acroporids towards Agariciids and Pocilloporids that were hypothesized (Raymundo et al., 2019). However, Raymundo et al. (2019) did note that these species replacements usually followed a bleaching event or disease outbreak, with correlations between disease and subsequent bleaching having been previously noted (Brandt & McManus, 2009). This indicates that high stress events may be the main contributor to this composition shift, which accelerates when high levels of whole colony mortality occur. Mortality is then followed by an

increase in non-living substrate that may then be utilized by stress tolerant and weedy coral species such as *Pavona decussata* and *Pocillopora damicornis*.

During the period of the study, August upper daily temperatures ranged around 31.5°C, which is well above the bleaching threshold of 29.9°C established for Guam's reefs from 1985-2003 (Burdick et al. 2008). However, bleaching was only observed in *Acropora pulchra* colonies that resided above the extreme low tide mark (Appendix Figure 2A), indicating that there is potential for island-wide acclimatization to higher water temperatures and potentially increased thermal tolerance (Barshis et al., 2010, Safaie et al., 2018). These results also may suggest that these higher temperatures were not the primary cause for bleaching, but rather, the effects of sub-aerial exposure during extreme low tides. This partial bleaching likely accounted for the decreases in overall coral cover and increases in non-living substrate and algae that were observed through our ecological monitoring (Figure 10 & 11). Additionally, because Guam's corals spawn in the summer months of May, June, and July (Richmond & Hunter, 1990), recruits from 2022's spawning event would have not been visible, as the recruits would have not had enough time to grow between the time of spawning and monitoring. Furthermore, qualitative historical evidence of long-term species replacement was observed when sampling, with many colonies of *Pavona decussata* growing over *Acropora pulchra* rubble from previous mortality events. This observation both indicates that long term community composition changes are occurring, and confirms *Pavona decussata*'s stress tolerance. (Appendix Figure 3A).

Although small scale temporal differences were not observed, reef community composition shifts across spatial scales were evident. Across Tanguisson and West Agaña, distinct differences within community composition was found. During the month of August, West Agaña Inner and Outer non-living substrate cover was 25% and 32.5%, respectively, while Tanguisson Inner and Outer non-living substrate cover accounted for nearly 50% of the reef (Figure 10). This higher

level of non-living substrate cover at Tanguisson may be due to a combination of factors, including White Syndrome (WS) disease outbreaks and extreme low tide events. These WS outbreaks have been shown to be more prevalent during the summer months in Tanguisson and are less prevalent within West Agaña *Acropora pulchra* populations (Greene et al., 2020), resulting in reduced *A. pulchra* populations across Tanguisson and creating large areas of non-living substrate dominated by *A. pulchra* rubble (Raymundo et al., 2019). Similarly, extreme low tide events are more prevalent in Tanguisson than in West Agaña, likely due to uneven tectonic submergence and emergence events (Randall & Eldredge, 1977; Randall, 1979). This trend is supported by the fact that the Tanguisson reef flat is shallower than West Agaña, resulting in higher levels of whole colony sub-aerial exposure in Tanguisson than in West Agaña.

2.2.2 Symbiont Community Diversity & Structure

Our results indicate that coral associated Symbiodiniaceae communities are structured by coral species and these associations are largely uniform across temporal and spatial scales (Figure 12). *Acropora pulchra*, *Pocillopora damicornis*, and *Pavona decussata* all retained their symbiont communities between February and August, indicating high levels of temporal stability regardless of season. *Pocillopora damicornis* and *Pavona decussata* Symbiodiniaceae assemblages were completely uniform across sites and zones, with *Durusdinium* lineages D1 and D2d comprising the Symbiodiniaceae communities of *P. damicornis*, and *Cladocopium* lineages C1 and C1c making up the Symbiodiniaceae communities of *P. decussata*. Within *Acropora pulchra*, Tanguisson Outer and West Agaña colonies were almost exclusively dominated by *Cladocopium* C40. This tight correlation between Symbiodiniaceae lineages and coral species is likely a factor of established, host-specific Symbiodiniaceae associations (Mote et al., 2021; Howe-Kerr et al., 2020; Bernasconi et al., 2019). However, Tanguisson Inner *Acropora pulchra* colonies displayed higher Symbiodiniaceae diversity, consisting primarily of *Durusdinium* D1, with smaller

signatures of *Durusdinium* D4 and *Cladocopium* C40 (Figure 12). This deviation from majority C40 lineages found across our other *Acropora pulchra* colonies may be an indication of environmentally induced selective pressures, resulting in more stress resilient Symbiodiniaceae (Claar et al., 2020; Cunning et al., 2015; LaJeunesse et al., 2010b). More broadly, *Durusdinium* D1/D4 and *Cladocopium* C40 have been previously identified as being able to withstand higher thermal regimes than other Symbiodiniaceae lineages (Claar et al., 2020; Qin, et al., 2019; LaJeunesse et al., 2014; Berkelmans & Van Oppen, 2006), suggesting that *Acropora pulchra* and *Pocillopora damicornis* associate with these stress tolerant Symbiodiniaceae in order to increase their survivorship and fitness. Interestingly, the absence of stress tolerant Symbiodiniaceae found within *Pavona decussata* further highlights *P. decussata*'s ability to modulate stress via host induced ROS scavenging or by other means in a greater capacity than the competitive *Acropora pulchra* or weedy *Pocillopora damicornis*.

2.2.3 Symbiodiniaceae Autofluorescent Dynamics

Within *Acropora pulchra* and *Pocillopora damicornis* associated Symbiodiniaceae, increases in antioxidant associated RFIs were observed from February to August before decreasing in November to near February levels (Figure 14). This trend indicates that colonies upregulated their photo-protective mechanisms during the summer months and downregulated their photo-protective mechanisms in the winter, which was also observed for Peridinin and Chlorophyll LHC RFIs. (Figure 15). This co-regulation between Symbiodiniaceae photopigments and photoprotective mechanisms in *Acropora pulchra* and *Pocillopora damicornis* likely illustrates shifting acclimatization processes that are divided between the hotter, wetter summer months that are characterized by reduced water flow dynamics and the cooler, drier winter months that are characterized by increased water flow dynamics. Furthermore, increases in photosynthesis during the summer months correlate with increases in temperature and light exposure, either from low

tide events or from reduced water flow. As light exposure increases, photosynthetic by-products such as ROS increase, which damage the photosynthetic apparatus (Niyogi, 1999). If the rate of ROS damage outweighs the rate of repair from antioxidant production, photoinhibition occurs (Niyogi, 1999), which is likely why we see a peak in the upregulation of Peridinin and Chlorophyll LHCs RFIs and antioxidant associated RFIs during summer months (May and August) (Figures 14 & 15). Seasonal acclimatization has been shown in other photosynthetic organisms (Kolari et al., 2014; Porcar-Castell et al., 2008, Mäkelä et al., 2004), suggesting that this may be an efficient mechanism to deal with fluctuations in temperatures and light across seasons. However, this trend was not identified within *Pavona decussata* associated Symbiodiniaceae, where antioxidant associated RFIs stayed consistently low across summer and winter months, while Peridinin and Chlorophyll LHC RFIs increased in the summer months and decreased in the winter months (Figures 14 & 15). This divergence between photopigments and photoprotective mechanisms in *Pavona decussata* may indicate host mediated photosystem regulation in addition to potential symbiont driven strategies to aid in reducing ROS build up via effective ROS scavenging. During August sample collection, we also observed that most *Pocillopora damicornis* colonies experienced whole colony mortality (Figure 11). As such, *Pocillopora damicornis*' Peridinin and Chlorophyll LHC RFI expression changed, resulting in a negative slope for August and signifies a breakdown of *P. damicornis*' LHC in response to stress induced mortality (Figure 15). *Pocillopora damicornis* was also found to have highly variable RFIs between colonies, sites, and when compared against *Acropora pulchra* and *Pavona decussata*'s fluorescence (Figures 14 & 15). We believe this may be attributed to potential differences between *Durusdinium* and *Cladocopium*'s gene expression and photophysiology (Cantin et al., 2009; Yuyama et al., 2018). Additionally, due to *Pocillopora damicornis*' large variations in morphology, high variability in colony photophysiology may also be due to an unresolved species complex, with different

subspecies of *Pocillopora* reacting differently to the environmental conditions observed on the reef flat.

Our results also highlighted differences in photosystem regulation between Symbiodiniaceae found in Tanguisson and West Agaña corals. Antioxidant associated RFIs in Tanguisson *Acropora pulchra* associated Symbiodiniaceae were found to increase between February and August, but stayed consistently high in West Agaña *A. pulchra* (Figure 14). By November, the antioxidant associated RFIs at both sites decreased drastically. However, even though West Agaña *Acropora pulchra*'s antioxidant associated RFIs stayed consistent between February and August, their signatures were significantly higher than in Tanguisson *A. pulchra* associated Symbiodiniaceae, regardless of the sampling month (Figure 14). Interestingly, this site distinction was not as apparent in *Pocillopora damicornis* associated Symbiodiniaceae and was entirely absent in *Pavona decussata* associated Symbiodiniaceae (Figure 14). These differences further emphasize LHC differences across species and sites, and highlights *Acropora pulchra*'s pattern of site-specific acclimatization while *Pocillopora damicornis* and *Pavona decussata* maintain similar RFIs across sites. Furthermore, given that the role of antioxidants includes the reduction of stress accumulation within Symbiodiniaceae, differences in these RFIs across sites may suggest that Tanguisson and West Agaña have differing water qualities and water flow dynamics. This hypothesis is supported by our current loggers, which revealed that Tanguisson has higher water flow (Figure 9), likely due to how narrow the reef flat is in comparison to West Agaña's reef flat, which allows Tanguisson to have greater mixing. Additionally, Tanguisson's reef flat is much farther from human development and the shore is entirely vegetated, whereas West Agaña is very close in proximity to human developments and drainage ditches (Figure 4), allowing for runoff and other pollutants to enter the water column.

2.2.4 Symbiodiniaceae Densities

Symbiodiniaceae densities within *Acropora pulchra*, *Pocillopora damicornis*, and *Pavona decussata* were found to significantly vary across species (Figure 13). This variability suggests that *Pavona decussata*'s high Symbiodiniaceae densities compared to that of *Acropora pulchra* and *Pocillopora damicornis* may be indicative of tissue layer and polyp size differences between species (Hill et al., 2012; Stimson et al., 2002). This correlates well with Stimson et al. (2002) and Warner et al. (1999), who suggest that species with low mortality rates have higher densities of Symbiodiniaceae, allowing Symbiodiniaceae to shade each other and provide protection from light induced stress. Additionally, *Pocillopora damicornis*'s low Symbiodiniaceae densities compared to *Acropora pulchra* and *Pavona decussata* may be an indication of a more heterotrophic lifestyle (Kisten 2013; Toh et al., 2013), which reduces the need for photosynthetic Symbiodiniaceae.

Differences in Symbiodiniaceae densities were also observed over time, with *Acropora pulchra* reducing its Symbiodiniaceae densities in the summer months, while *Pocillopora damicornis* and *Pavona decussata* slightly increased their Symbiodiniaceae densities during the same period (Figure 13). This decrease in *Acropora pulchra*'s Symbiodiniaceae densities was likely due to the paling of *A. pulchra* in May and August, which is a response to increased light induced stress. This phenomenon has been shown prior to this study (Jandang et al., 2022), and paling is an effective measure in reducing stress from photosynthetically induced ROS build-up. Furthermore, *Pavona decussata*'s and *Pocillopora damicornis*' increase in Symbiodiniaceae densities may be attributable to greater ROS-scavenging enzymatic processes within their Symbiodiniaceae – a proven strategy in reducing light damage (Murage & Masuda, 1997) within plants – which allowed them to maintain and even increase their Symbiodiniaceae densities. However, although the increases in *Pavona decussata*'s Symbiodiniaceae densities in the summer months points towards the innate stress tolerance found within the host, *Pocillopora damicornis*' Symbiodiniaceae increases are puzzling. A possible explanation for this is that *Pocillopora*

damicornis colonies harbored *Durusdinium* (Figure 12), which allowed for an increase in Symbiodiniaceae densities due to *Durusdinium*'s stress tolerant nature as well as its smaller size in comparison to *Cladocopium* (LaJeunesse et al., 2018). Regardless, we see that they did not follow *Acropora pulchra*'s reduction in cell densities, prompting the need for future investigation.

Along with temporal and species differences, spatial differences between Tanguisson and West Agaña's Symbiodiniaceae densities were observed, with Tanguisson corals harboring more Symbiodiniaceae than in West Agaña (Figure 13). This may be due to a combination of factors that stem from water flow dynamics. While sampling and collecting loggers across all our timepoints, we noticed that the increased water flow and wave action at Tanguisson correlated with increased amounts of bubble related turbidity, which was not observed in West Agaña. Due to this turbidity at Tanguisson, we believe that there may be an increased amount of shading within the water column due to the refraction of incoming light, thus reducing light intensities and increasing the amount of Symbiodiniaceae found within our Tanguisson corals. Additionally, given West Agaña's proximity to human developments and drainage culverts (Figure 4), the likelihood of increased nutrient runoff within West Agaña is high, which may result in increased dissolved nutrients within the water column. Higher nutrient loads may have resulted in West Agaña corals adapting to more heterotrophic conditions than their Tanguisson counterparts, reducing the need for photosynthetic Symbiodiniaceae, and thus, reducing their densities. This is supported by research that has described *Pocillopora* and *Pavona* as being heterotrophic and mixotrophic, respectively (Kisten 2013; Toh et al., 2013; Conti-Jerpe et al., 2020). However, *Acropora* has been previously described as autotrophic (Conti-Jerpe et al., 2020), potentially ruling out this theory. West Agaña corals may also have lower Symbiodiniaceae densities due to biological limitations within the boundary layer of corals. This boundary layer is integral in allowing solute diffusion between the water column and the coral (Nakamura & Van Woesik,

2001), a process facilitated by increased water flow. In corals found in areas of lower water flow (i.e., West Agaña (Figure 9)), metabolic by-products such as ROS may accumulate in the boundary layer, leading to stress responses from increases in light and temperature. However, the opposite occurs in areas of high water flow (i.e., Tanguisson (Figure 9)) (Nakamura & Van Woesik, 2001), allowing the rate of metabolic by-product expulsion to increase, which allows for greater photosynthetic maximums and a reduced need for antioxidant production. This reduced level of Symbiodiniaceae densities may also be due to differences in polyp morphology across sites, which can change how light is scattered within the skeleton of the coral (Enríquez et al., 2017). These differences between West Agaña and Tanguisson may have induced plasticity differences within the coral skeleton, creating light scattering properties within their skeletons and thus require these corals to have lower Symbiodiniaceae densities.

2.3 Conclusions

Through a combination of ecological, genetic, and physiological techniques, this project provided a detailed assessment of the mechanisms driving coral community composition shifts on Guam's reef flats. Our findings illuminate the ways in which different life history strategies are both correlated with and driven by specific biological mechanisms, while also revealing spatial differences in community compositions and environmental conditions that either accelerate or reduce the likelihood of species replacement. Our analysis has also highlighted how changes in temperature, low tide exposure, and water flow can have significant effects on the species that inhabit Guam's reef flats, and how the interplay between different factors can drive community composition shifts. Specifically, we found that *Acropora pulchra*, *Pocillopora damicornis*, and *Pavona decussata* all associate with different Symbiodiniaceae communities that are geographically stable, apart from Tanguisson Inner *Acropora pulchra*, which displayed different

Symbiodiniaceae communities than *A. pulchra* colonies in Tanguisson Outer and West Agaña. These results partially supports our second hypothesis, which stated that Symbiodiniaceae assemblage differences would be observed across spatial and species scales. Our analysis of Symbiodiniaceae cellular densities and autofluorescent signatures also captured unique species differences, highlighting *Pavona decussata*'s stress tolerant capabilities compared to that of *Acropora pulchra* and *Pocillopora damicornis*. Seasonal photoacclimation trends across all three coral species were also identified. This partially supports our third hypothesis, as differences in Symbiodiniaceae functionality were observed across temporal and spatial scales for all species, but at different magnitudes, with *Pavona decussata* having the most consistent Symbiodiniaceae functionality across time and space. Additionally, our findings did not show that *Pocillopora damicornis* had consistent Symbiodiniaceae functionality, instead acting more like *Acropora pulchra*'s Symbiodiniaceae than *Pavona decussata*'s. Furthermore, although our first hypothesis was not supported through our ecological monitoring due to the short timescale of this study, samples collected across multiple timepoints provided historical evidence that supported the argument for long-term species replacement, bolstering our assertion that *Pavona decussata* is better adapted to changing environments as compared to *Acropora pulchra*. This also suggests that community composition shifts on the reef flats of Guam are part of a recent, but ongoing, process of ecological change amidst climate change, whereby the competitive Acroporid is being outcompeted by weedy Pocilloporids and stress tolerant Agariciids. These findings have important implications for understanding what coral communities will look like in the future, why coral species respond to environmental stressors, and how they may adapt to changing conditions in the future. By focusing on these three corals, our research sheds light on the nuanced differences within each species, contributing to a deeper understanding of the factors shaping coral reef

ecosystems. This knowledge is essential for developing effective conservation strategies that can help protect and preserve these important and vulnerable ecosystems for future generations.

Temperature Data

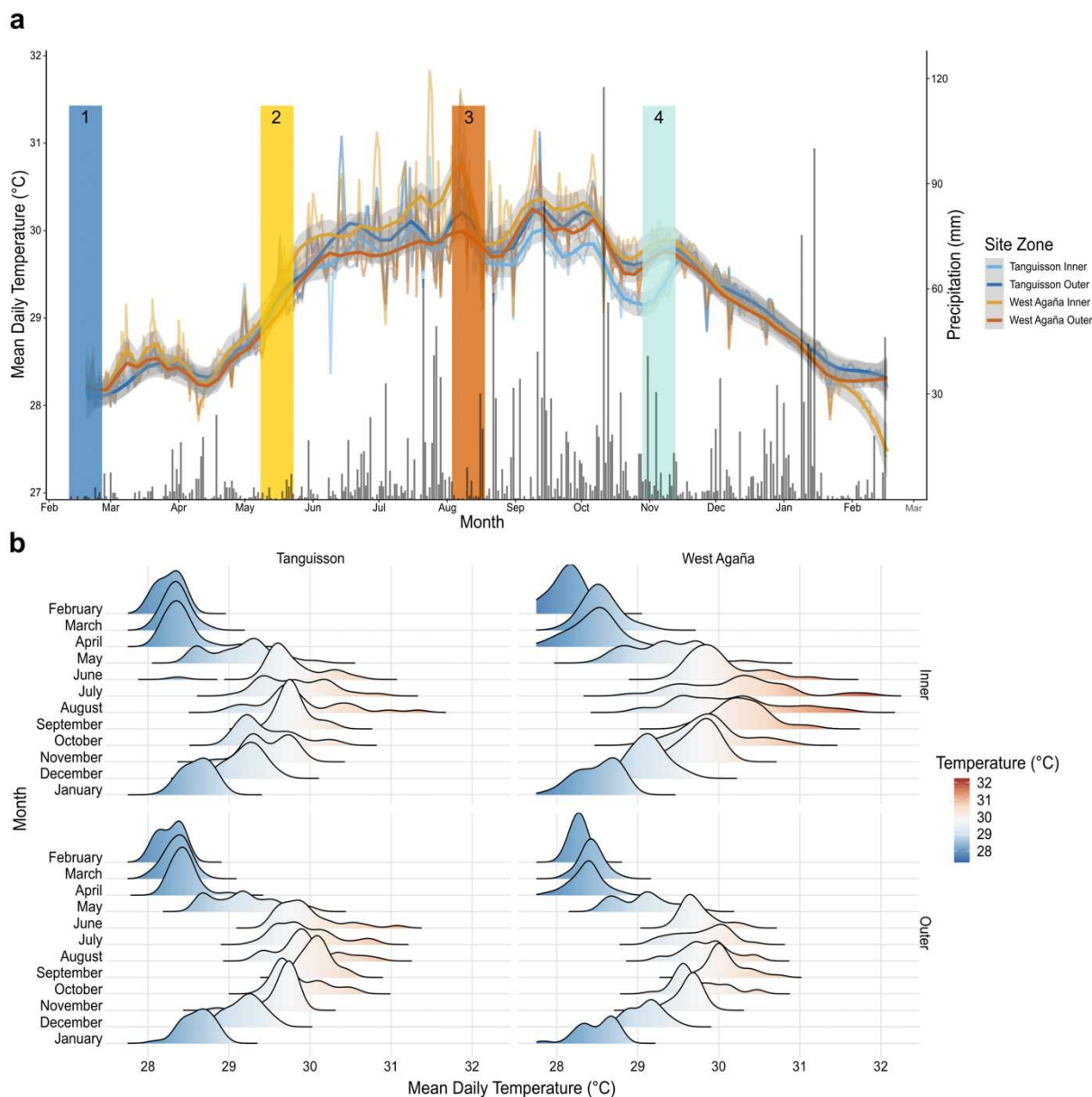


Figure 8: **a)** Mean daily sea surface temperatures (SST) for each site zone captured by Onset HOBO temperature loggers across 12-month period (February 2022-2023) overlaid with precipitation data from the same period collected by Menne et al., 2012. Sample collections were completed in February (blue, pre-warming period), May (yellow, transitional pre-warming period), August (orange, peak warming period), November (light blue, transitional post-warming period), and are shown by the blue, yellow, orange, and light teal bars. **b)** Distribution of mean daily SSTs across the 12-month period (February 2022-2023) illustrating differences in extremes between Inner and Outer zones for each site.

Current Data

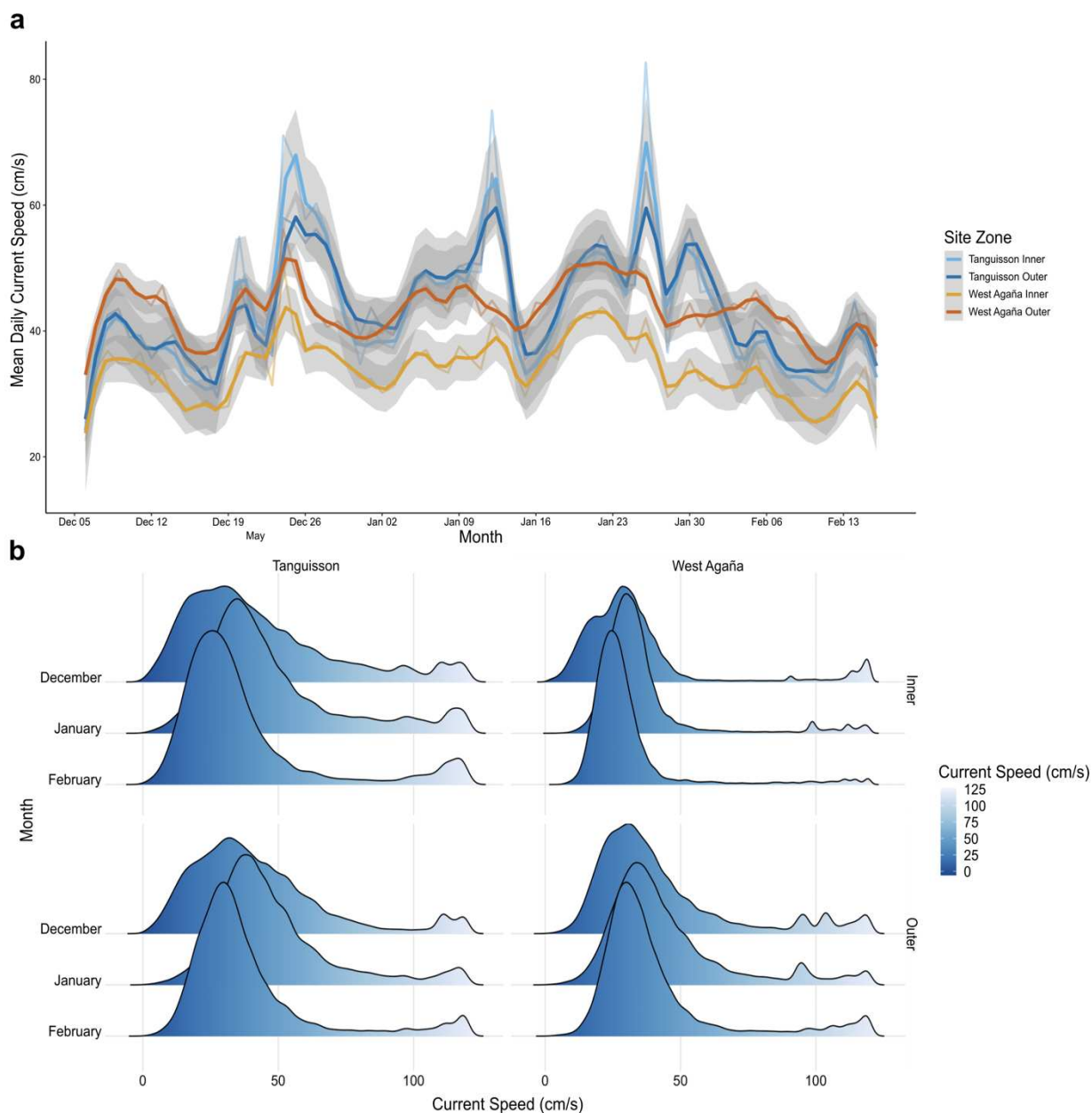


Figure 9: **a)** Mean daily current speed (cm/s) for each site and zone captured by TCM-4 Shallow water Tilt Current Meters across a 3-month period (December 2022-February 2023). **b)** Distribution of mean daily current speed (cm/s) across 3-month period (December 2022-February 2023) illustrating differences in extremes between the inner and outer zones for each site.

Ecological Monitoring Data

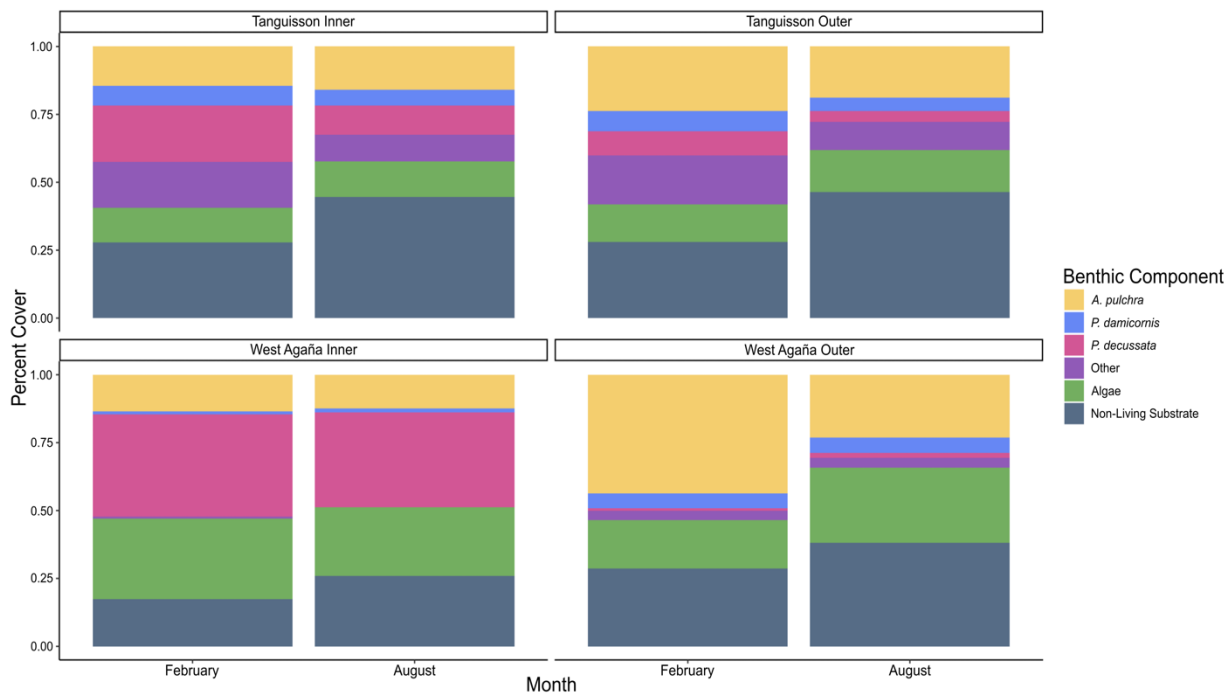


Figure 10: Stacked bar plot showing percent coverage of benthic components across site zones: *Acropora pulchra* (*A. pulchra*), *Pocillopora damicornis* (*P. damicornis*), *Pavona decussata* (*P. decussata*), Other coral species (Other), Algae, and Non-Living Substrate. Surveys were conducted in February (pre-warming period) and August (peak warming period).

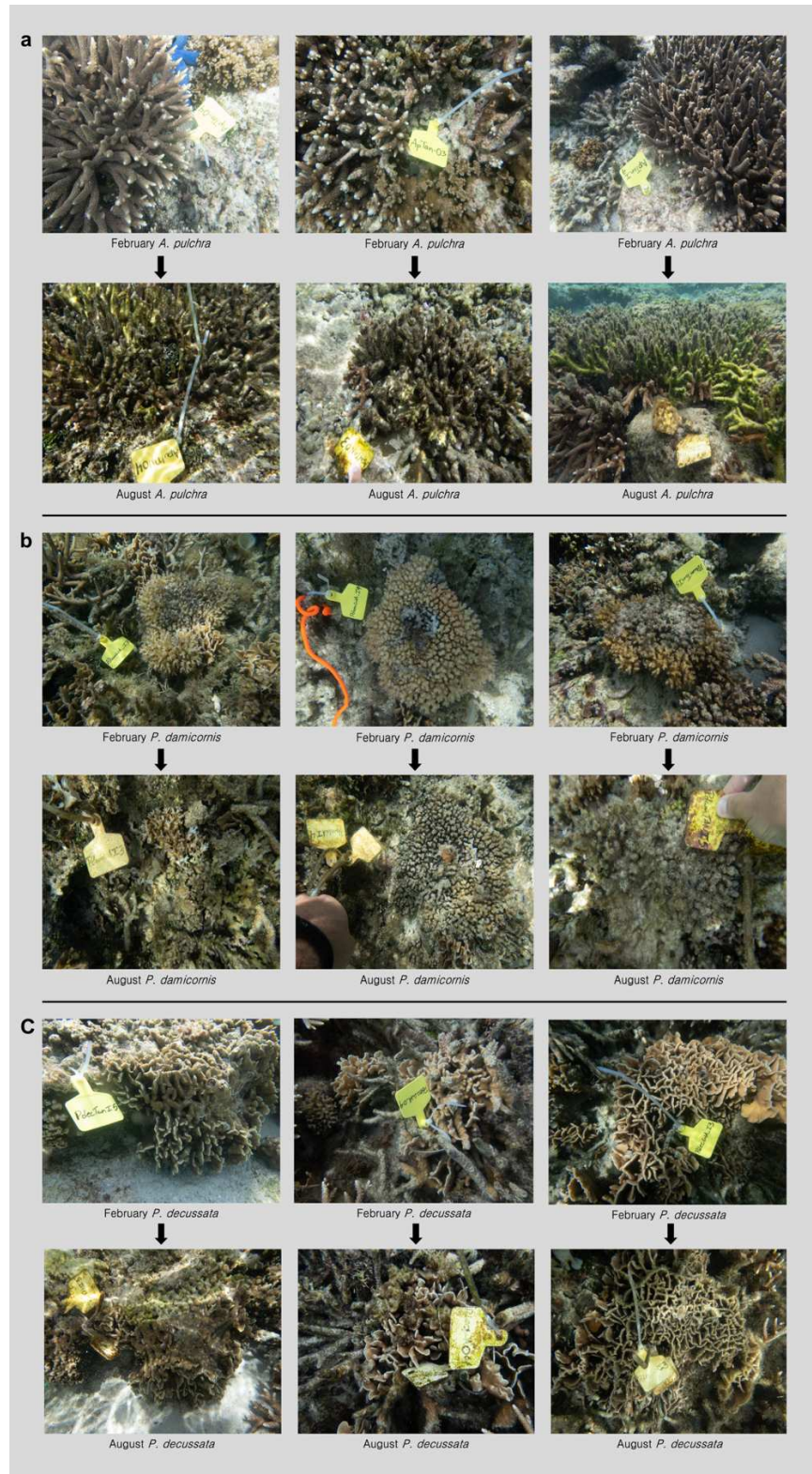


Figure 11: Photographs taken of tagged **a) *Acropora pulchra***, **b) *Pocillopora damicornis***, and **c) *Pavona decussata*** coral colonies during ecological monitoring surveys in February (pre-warming period) and August (peak warming period).

Symbiodiniaceae Community Data

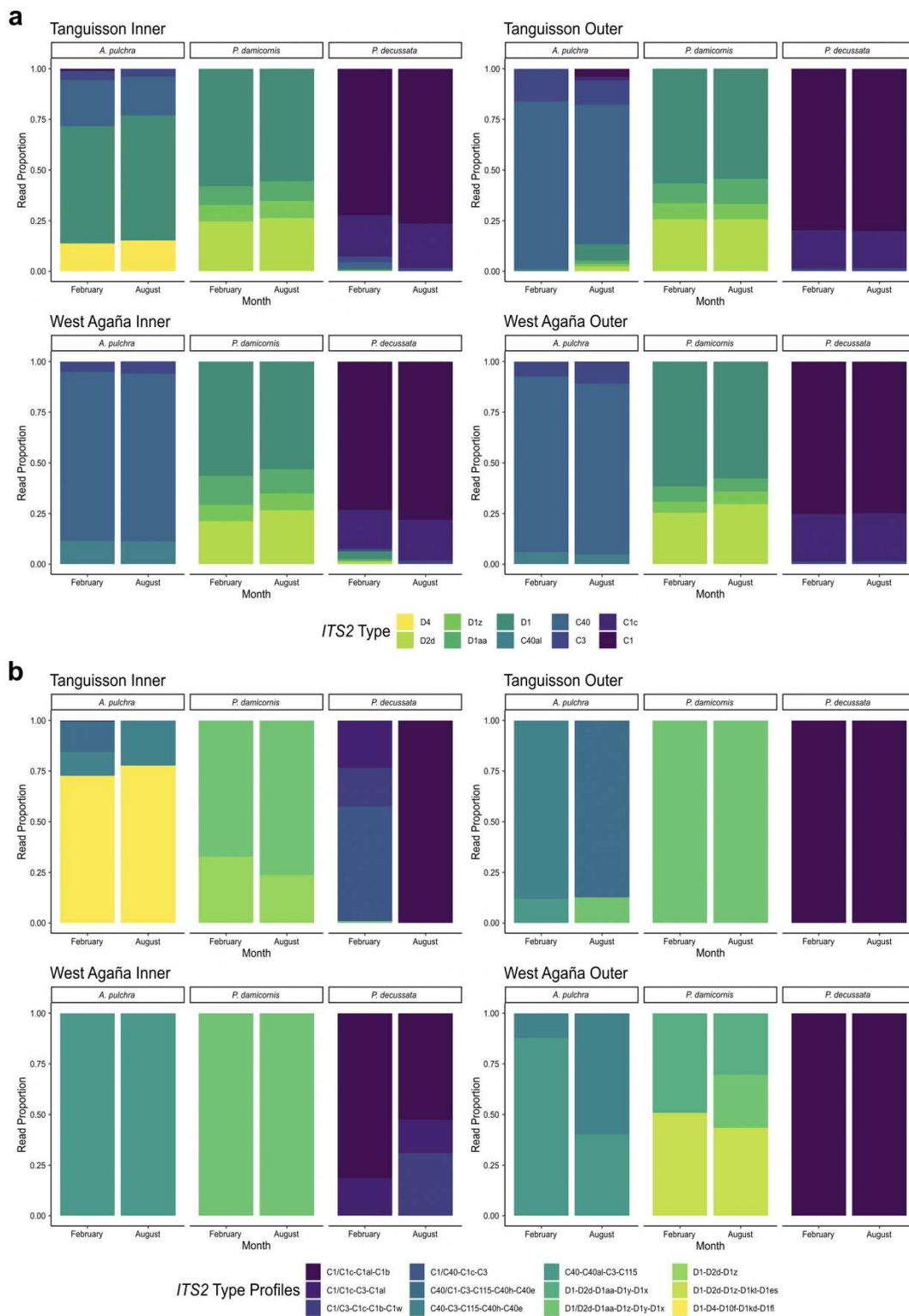


Figure 12: a). *ITS2* type and type profile diversity for coral associated Symbiodiniaceae found within tagged *Acropora pulchra*, *Pocillopora damicornis*, and *Pavona decussata* colonies for each site and zone across time.

Symbiodiniaceae Density Data

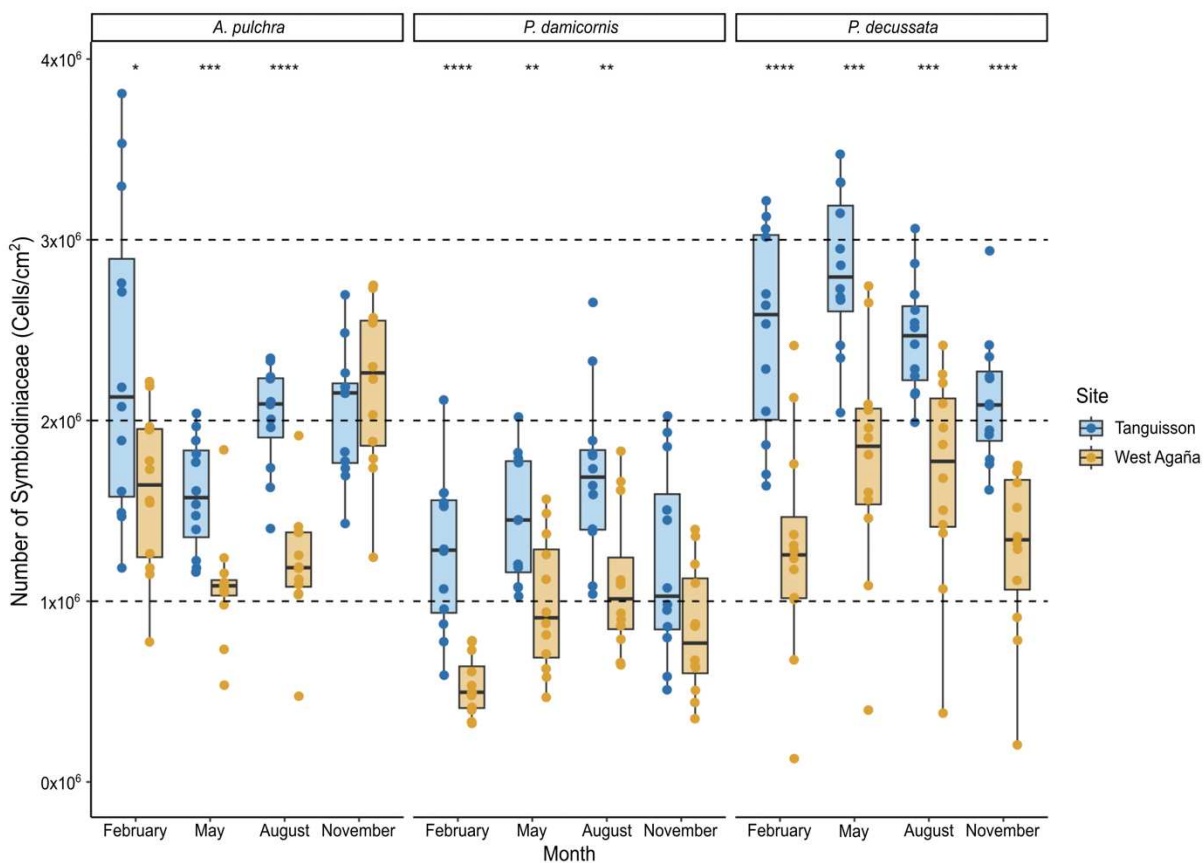


Figure 13: Symbiodiniaceae densities (cells/cm²) for *Acropora pulchra*, *Pocillopora damicornis*, and *Pavona decussata* in February (pre-warming period), May (transitional pre-warming period), August (peak warming period), and November (transitional post-warming period) for Tanguisson (blue) and West Agaña (orange). Points represent average RFI contributions for each colony collected. Stars represent significance level.

Symbiodiniaceae Fluorescence Data

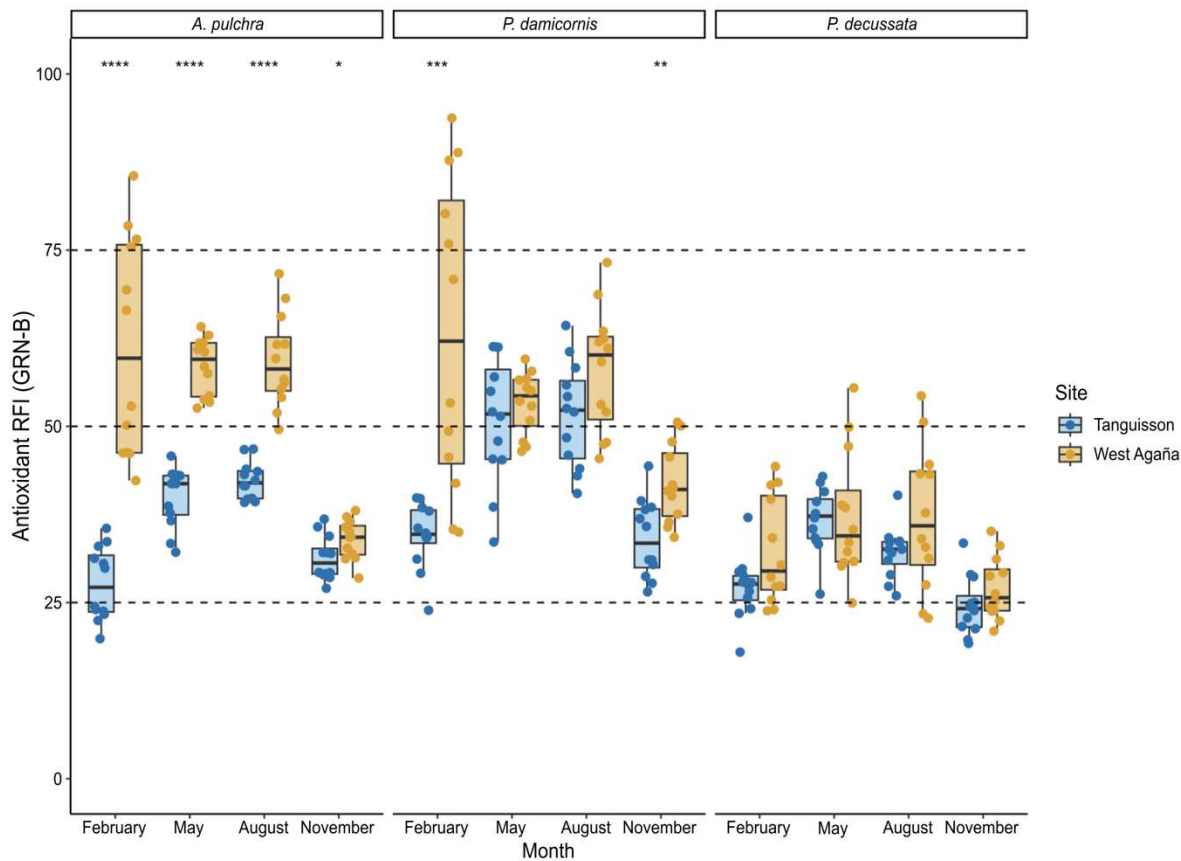


Figure 14: Symbiodiniaceae Relative Fluorescent Intensity (RFI) for antioxidant associated fluorescent proteins. Samples were analyzed from tagged *Acropora pulchra*, *Pocillopora damicornis*, and *Pavona decussata* colonies that were collected in February (pre-warming period), May (transitional pre-warming period), August (peak warming period), and November (transitional post-warming period) for Tanguisson (blue) and West Agaña (orange). Points represent average RFI contributions for each colony collected. Stars represent significance level.

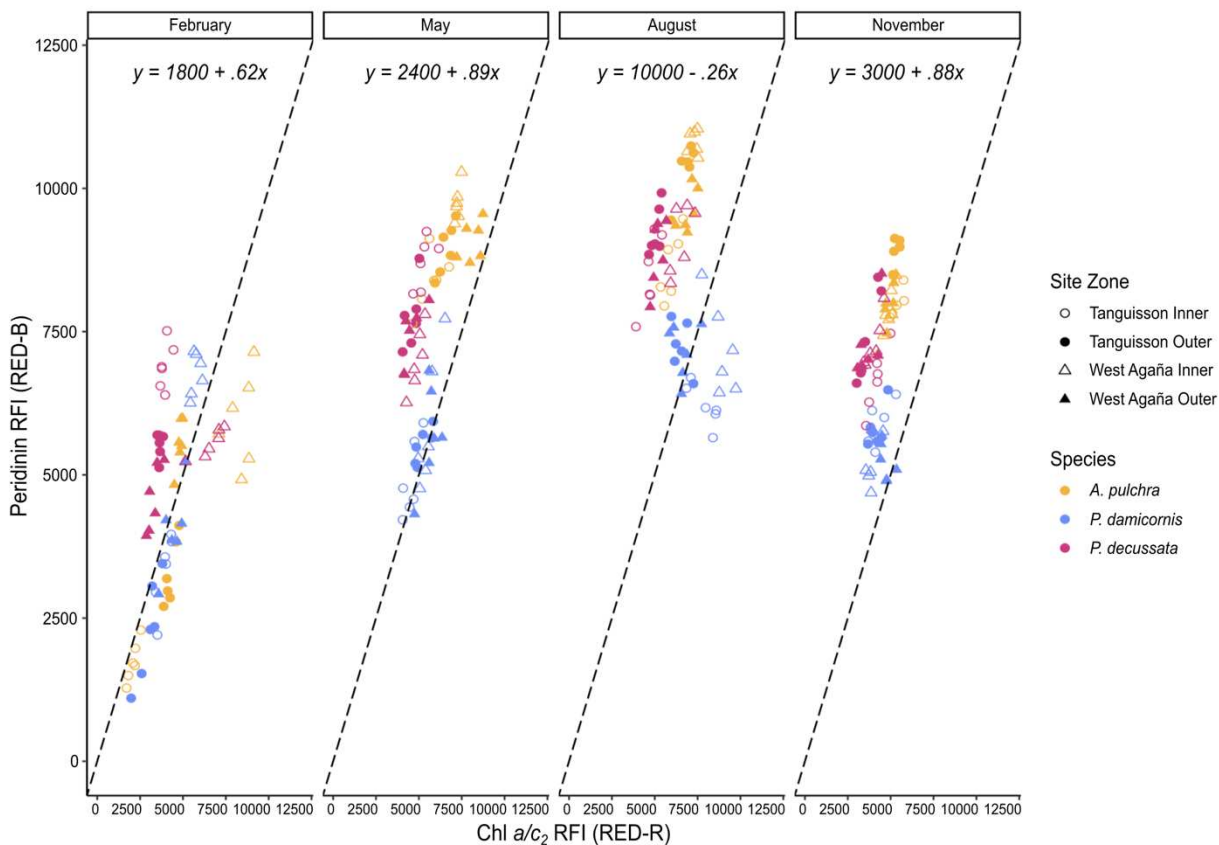


Figure 15: Peridinin – chlorophyll associated RFI ratios for *Acropora pulchra* (yellow), *Pocillopora damicornis* (blue), and *Pavona decussata* (pink) across February (pre-warming period), May (transitional pre-warming period), August (peak warming period), and November (transitional post-warming period) for sites and zones. Linear regression equations indicate peridinin – chlorophyll ratios, while dotted lines indicate 1:1 relationship for reference.

Table 1: Series of Repeated Measures - MANOVAs determining which factors contributed to physiological variation in cellular density, peridinin, chlorophyll, and antioxidant associated RFI, over time, site, zone, and species.

	Cellular Density			Peridinin		
	F	df	p	F	df	p
Time	2.905	3	0.036	902.138	3	< 0.001
Site	78.841	1	< 0.001	27.557	1	< 0.001
Zone	2.444	1	0.123	0.732	1	0.396
Species	45.452	2	< 0.001	266.210	2	< 0.001
Site:Zone	0.145	1	0.705	26.331	1	< 0.001
Site:Species	2.878	2	0.0641	28.254	2	< 0.001
Zone:Species	3.302	2	0.0436	4.586	2	0.01401
Site:Zone:Species	1.993	2	0.1452	9.152	2	< 0.001
Time:Site	6.755	3	0.000242	51.894	3	< 0.001
Time:Zone	5.583	3	0.001103	22.728	3	< 0.001
Time:Species	22.310	6	< 0.001	76.155	6	< 0.001
Time:Site:Zone	2.009	3	0.114380	7.908	3	< 0.001
Time:Site:Species	2.651	6	0.017292	40.027	6	< 0.001
Time:Zone:Species	3.237	6	0.004804	11.855	6	< 0.001
Time:Site:Zone:Species	1.757	6	0.110428	4.255	6	< 0.001
	Chlorophyll			Antioxidant		
	F	df	p	F	df	p
Time	353.091	3	< 0.001	162.686	3	< 0.001
Site	162.182	1	< 0.001	267.080	1	< 0.001
Zone	41.502	1	< 0.001	1.874	1	0.176
Species	131.174	2	< 0.001	225.430	2	< 0.001
Site:Zone	58.313	1	< 0.001	26.430	1	< 0.001
Site:Species	15.01	2	< 0.001	40.353	2	< 0.001

Zone:Species	16.83	2	< 0.001	21.645	2	< 0.001
Site:Zone:Species	11.50	2	< 0.001	25.577	2	< 0.001
Time:Site	71.89	3	< 0.001	57.408	3	< 0.001
Time:Zone	36.28	3	< 0.001	17.203	3	< 0.001
Time:Species	44.56	6	< 0.001	6.203	6	< 0.001
Time:Site:Zone	49.82	3	< 0.001	6.974	3	< 0.005
Time:Site:Species	14.60	6	< 0.001	16.338	6	< 0.001
Time:Zone:Species	11.73	6	< 0.001	16.342	6	< 0.001
Time:Site:Zone:Species	13.12	6	< 0.001	30.348	6	< 0.001

Table 2: Series of Kruskal-Wallis nonparametric tests to determine contributions to Ecological Monitoring data via time, site, zone, benthic component, and non-coral vs coral comparisons; Temperature data via time, site, and zone; and Rainfall data via time comparisons. Contributions to Current Speed data were discovered using ANOVAs via time, site, and zone comparisons.

	Percent Cover			Abundance		
	χ^2	df	p	χ^2	df	p
Time	0.372	1	0.542	1.214	1	0.271
Site	9.673	1	0.002	5.718	1	0.017
Zone	0.024	1	0.877	0.076	1	0.782
Benthic Component	350.512	5	< 0.001	607.510	5	< 0.001
Non-Coral vs Coral	202.290	1	< 0.001	274.130	1	< 0.001
Site:Zone	9.704	3	0.021	5.883	3	0.118
	Temperature			Current Speed		
	χ^2	df	p	F	df	p
Time	345.814	3	< 0.001	63.659	2	< 0.001
Site	0.438	1	0.508	77.096	1	< 0.001
Zone	0.002	1	0.961	104.023	1	< 0.001
Site:Zone	4.342	3	0.227	79.836	1	< 0.001
	Rainfall					
	χ^2	df	p			
Time	12.905	3	0.005			

Table 3: Series of Pairwise Adonis for Symbiodiniaceae ITS2 Types.

	Comparison	ITS2 Type		
		F	R²	p
Time	February vs August	1.726	0.012	0.109
Site	Tanguisson vs West Agaña	2.731	0.019	0.021
Zone	Inner vs Outer	1.948	0.014	0.075
Species	<i>A. pulchra</i> vs <i>P. damicornis</i>	59.227	0.387	< 0.001
	<i>A. pulchra</i> vs <i>P. decussata</i>	23.118	0.197	< 0.001
	<i>P. damicornis</i> vs <i>P. decussata</i>	92.028	0.495	< 0.001
Site:Zone	Tanguisson Inner vs Tanguisson Outer	2.957	0.041	0.0320
	Tanguisson Inner vs West Agaña Inner	4.256	0.057	0.008
	Tanguisson Inner vs West Agaña Outer	4.110	0.055	0.008
	Tanguisson Outer vs West Agaña Inner	0.842	0.012	0.559
	Tanguisson Outer vs West Agaña Outer	0.777	0.011	0.559
	West Agaña Inner vs West Agaña Outer	1.166	0.016	0.460

Table 4: Series of Pairwise Adonis for Symbiodiniaceae ITS2 Types via species and site:zone specific to each coral species.

Site:Zone	Comparison	<i>Acropora pulchra</i>			<i>Pocillopora damicornis</i>			<i>Pavona decussata</i>		
		F	R ²	p	F	R ²	p	F	R ²	p
	Tanguisson Inner vs Tanguisson Outer	13.838	0.386	< 0.001	0.757	0.033	0.576	0.892	0.039	0.406
	Tanguisson Inner vs West Agaña Inner	18.335	0.455	< 0.001	1.348	0.058	0.406	3.763	0.146	0.078
	Tanguisson Inner vs West Agaña Outer	19.604	0.471	< 0.001	0.891	0.039	0.513	2.578	0.105	0.101
	Tanguisson Outer vs West Agaña Inner	0.966	0.042	0.432	1.903	0.080	0.406	2.296	0.094	0.169
	Tanguisson Outer vs West Agaña Outer	1.202	0.052	0.403	1.302	0.056	0.406	1.682	0.071	0.169
	West Agaña Inner vs West Agaña Outer	0.277	0.012	0.785	1.728	0.073	0.406	4.686	0.176	0.075

2.4 References

- Ahmad, M., & Cashmore, A. R. (1993). HY4 gene of *A. thaliana* encodes a protein with characteristics of a blue-light photoreceptor. *Nature*, *366*(6451), 162-166.
- Anthony, C. J., Lock, C. C., & Bentlage, B. (2022). High-throughput physiological profiling of endosymbiotic dinoflagellates (Symbiodiniaceae) using flow cytometry. *bioRxiv*, 2022-12.
- Anthony, K. R. N., & Kerswell, A. P. (2007). Coral mortality following extreme low tides and high solar radiation. *Marine Biology*, *151*(5), 1623-1631.
- Aronson, R. B., & Precht, W. F. (1997). Stasis, biological disturbance, and community structure of a Holocene coral reef. *Paleobiology*, *23*(3), 326-346.
- Atkinson M., Falter J., Hearn C. (2001). Nutrient dynamics in the Biosphere 2 coral reef mesocosm: water velocity controls NH₄ and PO₄ uptake. *Coral Reefs*, *20*(4), 341–346. <https://doi.org/10.1007/s00338-001-0184-7>
- Babcock, R. C., Bull, G. D., Harrison, P. L., Heyward, A. J., Oliver, J. K., Wallace, C. C., & Willis, B. L. (1986). Synchronous spawnings of 105 scleractinian coral species on the Great Barrier Reef. *Marine Biology*, *90*(3), 379-394.
- Baker, A. C. (2003). Flexibility and specificity in coral-algal symbiosis: diversity, ecology, and biogeography of Symbiodinium. *Annual Review of Ecology, Evolution, and Systematics*, 661-689.
- Baker, D. M., Andras, J. P., Jordán-Garza, A. G., & Fogel, M. L. (2013). Nitrate competition in a coral symbiosis varies with temperature among Symbiodinium clades. *The ISME journal*, *7*(6), 1248-1251.
- Barshis, D. J., Stillman, J. H., Gates, R. D., Toonen, R. J., Smith, L. W., & Birkeland, C. (2010). Protein expression and genetic structure of the coral *Porites lobata* in an environmentally extreme Samoan back reef: does host genotype limit phenotypic plasticity?. *Molecular ecology*, *19*(8), 1705-1720.
- Bautista, J. A., Hiller, R. G., Sharples, F. P., Gosztola, D., Wasielewski, M., & Frank, H. A. (1999). Singlet and Triplet Energy Transfer in the Peridinin–Chlorophyll a–Protein from Amphidinium c. arerae. *The Journal of Physical Chemistry A*, *103*(14), 2267-2273.
- Bayraktarov, E., Pizarro, V., Eidens, C., Wilke, T., & Wild, C. (2013). Bleaching susceptibility and recovery of Colombian Caribbean corals in response to water current exposure and seasonal upwelling. *PloS one*, *8*(11), e80536.

- Berg, J. T., David, C. M., Gabriel, M. M., & Bentlage, B. (2020). Fluorescence signatures of persistent photosystem damage in the staghorn coral *Acropora cf. pulchra* (Anthozoa: Scleractinia) during bleaching and recovery. *Marine Biology Research*, 16(8-9), 643-655.
- Berkelmans, R., & Van Oppen, M. J. (2006). The role of zooxanthellae in the thermal tolerance of corals: a 'nugget of hope' for coral reefs in an era of climate change. *Proceedings of the Royal Society B: Biological Sciences*, 273(1599), 2305-2312.
- Bernasconi, R., Stat, M., Koenders, A., & Huggett, M. J. (2019). Global networks of Symbiodinium-bacteria within the coral holobiont. *Microbial ecology*, 77(3), 794-807.
- Boyett, H. V., Bourne, D. G., & Willis, B. L. (2007). Elevated temperature and light enhance progression and spread of black band disease on staghorn corals of the Great Barrier Reef. *Marine Biology*, 151(5), 1711-1720.
- Brandt, M. E., & McManus, J. W. (2009). Disease incidence is related to bleaching extent in reef-building corals. *Ecology*, 90(10), 2859-2867.
- Briggs, W. R., & Huala, E. (1999). Blue-light photoreceptors in higher plants. *Annual review of cell and developmental biology*, 15(1), 33-62.
- Brown, B. E., Dunne, R. P., Scoffin, T. P., & Le Tissier, M. D. A. (1994a). Solar damage in intertidal corals. *Marine Ecology Progress Series*, 219-230.
- Brown, B. E., Le Tissier, M. D. A., & Dunne, R. P. (1994b). Tissue retraction in the scleractinian coral *Coeloseris mayeri*, its effect upon coral pigmentation, and preliminary implications for heat balance. *Marine Ecology-Progress Series*, 105, 209-209.
- Büchel, C. (2020). Light harvesting complexes in chlorophyll c-containing algae. *Biochimica et Biophysica Acta (BBA)-Bioenergetics*, 1861(4), 148027.
- Bujak, Ł., Piątkowski, D., Mackowski, S., Wörmke, S., Jung, C., Bräuchle, C., ... & Hiller, R. (2009). Plasmon Enhancement of Fluorescence in Single Light-Harvesting Complexes from *Amphidinium carterae*. *Acta Physica Polonica A*, 116(S).
- Buma, B., Bisbing, S., Krapek, J., & Wright, G. (2017). A foundation of ecology rediscovered: 100 years of succession on the William S. Cooper plots in Glacier Bay, Alaska. *Ecology*, 98(6), 1513-1523.
- Burke, L., Reytar, K., Spalding, M., & Perry, A. (2011). *Reefs at risk revisited*. World resources institute.

- Cantin, N. E., van Oppen, M. J., Willis, B. L., Mieog, J. C., & Negri, A. P. (2009). Juvenile corals can acquire more carbon from high-performance algal symbionts. *Coral Reefs*, *28*, 405-414.
- Claar, D. C., Tietjen, K. L., Cox, K. D., Gates, R. D., & Baum, J. K. (2020). Chronic disturbance modulates symbiont (Symbiodiniaceae) beta diversity on a coral reef. *Scientific reports*, *10*(1), 4492.
- Connell, J. H. (1978). Diversity in tropical rain forests and coral reefs: high diversity of trees and corals is maintained only in a nonequilibrium state. *Science*, *199*(4335), 1302-1310.
- Connell, J. H., & Slatyer, R. O. (1977). Mechanisms of succession in natural communities and their role in community stability and organization. *The american naturalist*, *111*(982), 1119-1144.
- Conti-Jerpe, I. E., Thompson, P. D., Wong, C. W. M., Oliveira, N. L., Duprey, N. N., Moynihan, M. A., & Baker, D. M. (2020). Trophic strategy and bleaching resistance in reef-building corals. *Science Advances*, *6*(15), eaaz5443.
- Cramer, K. L., Jackson, J. B., Angioletti, C. V., Leonard-Pingel, J., & Guilderson, T. P. (2012). Anthropogenic mortality on coral reefs in Caribbean Panama predates coral disease and bleaching. *Ecology letters*, *15*(6), 561-567.
- Cunning, R., Yost, D. M., Guarinello, M. L., Putnam, H. M., & Gates, R. D. (2015). Variability of Symbiodinium communities in waters, sediments, and corals of thermally distinct reef pools in American Samoa. *PLoS One*, *10*(12), e0145099.
- D'Amico-Damião, V., & Carvalho, R. F. (2018). Cryptochrome-related abiotic stress responses in plants. *Frontiers in plant science*, *9*, 1897.
- Damjanović, A., Ritz, T., & Schulten, K. (2000). Excitation transfer in the peridinin-chlorophyll-protein of *Amphidinium carterae*. *Biophysical journal*, *79*(4), 1695-1705.
- Darling, E. S., Alvarez-Filip, L., Oliver, T. A., McClanahan, T. R., & Côté, I. M. (2012). Evaluating life-history strategies of reef corals from species traits. *Ecology Letters*, *15*(12), 1378-1386.
- Deng, B., Jin, X., Yang, Y., Lin, Z., & Zhang, Y. (2014). The regulatory role of riboflavin in the drought tolerance of tobacco plants depends on ROS production. *Plant growth regulation*, *72*, 269-277.
- Dennison, W. C., & Barnes, D. J. (1988). Effect of water motion on coral photosynthesis and calcification. *Journal of Experimental Marine Biology and Ecology*, *115*(1), 67-77.

- Dollar, S. J. (1982). Wave stress and coral community structure in Hawaii. *Coral Reefs*, 1(2), 71-81.
- Done, T. J. (1982). Patterns in the distribution of coral communities across the central Great Barrier Reef. *Coral reefs*, 1(2), 95-107.
- Drepper, T., Eggert, T., Circolone, F., Heck, A., Krauss, U., Guterl, J. K., ... & Jaeger, K. E. (2007). Reporter proteins for in vivo fluorescence without oxygen. *Nature biotechnology*, 25(4), 443-445.
- Eakin, C., Donner, S. D., Logan, C. A., Gledhill, D. K., Liu, G., Heron, S. F., ... & Strong, A. E. (2010, December). Thresholds for coral bleaching: Are synergistic factors and shifting thresholds changing the landscape for management?. In *AGU Fall Meeting Abstracts* (Vol. 2010, pp. B32A-04).
- Emery, P., So, W. V., Kaneko, M., Hall, J. C., & Rosbash, M. (1998). CRY, a *Drosophila* clock and light-regulated cryptochrome, is a major contributor to circadian rhythm resetting and photosensitivity. *Cell*, 95(5), 669-679.
- Enríquez, S., Méndez, E. R., Hoegh-Guldberg, O., & Iglesias-Prieto, R. (2017). Key functional role of the optical properties of coral skeletons in coral ecology and evolution. *Proceedings of the Royal Society B: Biological Sciences*, 284(1853), 20161667.
- Ezzat, L., Fine, M., Maguer, J. F., Grover, R., & Ferrier-Pages, C. (2017). Carbon and nitrogen acquisition in shallow and deep holobionts of the scleractinian coral *S. pistillata*. *Frontiers in Marine Science*, 4, 102.
- Fawley, M. W. (1989). A new form of chlorophyll c involved in light-harvesting. *Plant physiology*, 91(2), 727-732.
- Falkowski, P. G., & Raven, J. A. (1997). Aquatic photosynthesis blackwell science. *Malden, Massachusetts*, 375.
- Fenner, D. (2021). Field Identification Guide to the Corals of the Mariana Archipelago, including Guam and the Commonwealth of the Northern Mariana Islands. Version 1.0.
- Fifer, J., Bentlage, B., Lemer, S., Fujimura, A. G., Sweet, M., & Raymundo, L. J. (2021). Going with the flow: How corals in high-flow environments can beat the heat. *Molecular Ecology*, 30(9), 2009-2024.
- Finelli, C. M., Helmuth, B. S., Pentcheff, N. D., & Wethey, D. S. (2006). Water flow influences oxygen transport and photosynthetic efficiency in corals. *Coral Reefs*, 25(1), 47-57.

- Foyer, C., and Noctor, G. (2003) Redox sensing and signalling associated with reactive oxygen in chloroplasts, peroxisomes and mitochondria. *Physiol Plant* 119: 355–364.
- Fujimura, A. G., & Riegl, B. M. (2017). Effects of water flow on intra-and intercolonial variability in bleaching of the zoanthid, *Palythoa caribaeorum*. *Journal of Experimental Marine Biology and Ecology*, 490, 29-33.
- Glynn, P. W. (1984). Widespread coral mortality and the 1982–83 El Niño warming event. *Environmental Conservation*, 11(2), 133-146.
- Goss, R., and Lepetit, B. (2015) Biodiversity of NPQ. *J Plant Physiol* 172: 13–32.
- Graham, N. A., Wilson, S. K., Jennings, S., Polunin, N. V., Bijoux, J. P., & Robinson, J. (2006). Dynamic fragility of oceanic coral reef ecosystems. *Proceedings of the National Academy of Sciences*, 103(22), 8425-8429.
- Greene, A., Donahue, M. J., Caldwell, J. M., Heron, S. F., Geiger, E., & Raymundo, L. J. (2020). Coral disease time series highlight size-dependent risk and other drivers of white syndrome in a multi-species model. *Frontiers in Marine Science*, 7, 601469.
- Greenstein, B. J., Curran, H. A., & Pandolfi, J. M. (1998). Shifting ecological baselines and the demise of *Acropora cervicornis* in the western North Atlantic and Caribbean Province: a Pleistocene perspective. *Coral Reefs*, 17(3), 249-261.
- Gressel, J. (1979). Blue light photoreception. *Photochemistry and photobiology*, 30(6), 749-754.
- Grigg, R. W. (1983). Community structure, succession and development of coral reefs in. *Marine Ecological Progress Series*, 11, 1-14.
- Grime, J. P. (1977). Evidence for the existence of three primary strategies in plants and its relevance to ecological and evolutionary theory. *The american naturalist*, 111(982), 1169-1194.
- Grime, J. P., & Pierce, S. (2012). *The evolutionary strategies that shape ecosystems*. John Wiley & Sons.
- Harrison, P. L., Babcock, R. C., Bull, G. D., Oliver, J. K., Wallace, C. C., & Willis, B. L. (1984). Mass spawning in tropical reef corals. *Science*, 223(4641), 1186-1189.
- Haubner, N., Sylvander, P., Vuori, K., and Snoeijs, P. (2014) Abiotic stress modifies the synthesis of alpha-tocopherol and beta-carotene in phytoplankton species. *J Phycol* 50: 753–759.

- Hayashibara, T., Ohike, S., & Kakinuma, Y. (1997). Embryonic and larval development and planula metamorphosis of four gamete-spawning *Acropora* (Anthozoa, Scleractinia). In *Proceedings of the 8th International Coral Reef Symposium, Panama* (Vol. 2, pp. 1231-1236).
- Helmuth, B. S. (1998). Intertidal mussel microclimates: predicting the body temperature of a sessile invertebrate. *Ecological Monographs*, 68(1), 51-74.
- Herlan, J., & Lirman, D. (2008, July). Development of a coral nursery program for the threatened coral *Acropora cervicornis* in Florida. In *Proc 11th Int coral reef symp* (Vol. 24, pp. 1244-1247).
- Heron, S. F., Raymundo, L., Sweet, W. V., Papa, A., Moreland-Ochoa, C., & Burdick, D. R. (2020). Predicting extreme tide events to inform shallow reef community restoration and management in Guam.
- Hill, R., Larkum, A. W. D., Prášil, O., Kramer, D. M., Szabó, M., Kumar, V., & Ralph, P. J. (2012). Light-induced dissociation of antenna complexes in the symbionts of scleractinian corals correlates with sensitivity to coral bleaching. *Coral Reefs*, 31, 963-975.
- Hiller, R. G., Wrench, P. M., Gooley, A. P., Shoebridge, G., & Breton, J. (1993). The major intrinsic light-harvesting protein of *Amphidinium*: Characterization and relation to other light-harvesting proteins. *Photochemistry and Photobiology*, 57(1), 125-131.
- Hoegh-Guldberg Ove (1999) Climate change, coral bleaching and the future of the world's coral reefs. *Marine and Freshwater Research* 50, 839-866.
- Hoegh-Guldberg, O., Poloczanska, E. S., Skirving, W., & Dove, S. (2017). Coral reef ecosystems under climate change and ocean acidification. *Frontiers in Marine Science*, 4, 158.
- Hoegh-Guldberg, O., & Smith, G. J. (1989). The effect of sudden changes in temperature, light and salinity on the population density and export of zooxanthellae from the reef corals *Stylophora pistillata* Esper and *Seriatopora hystrix* Dana. *Journal of Experimental Marine Biology and Ecology*, 129(3), 279-303.
- Hoegh-Guldberg, O., Mumby, P. J., Hooten, A. J., Steneck, R. S., Greenfield, P., Gomez, E., ... Hatziolos, M. E. (2007). Coral reefs under rapid climate change and ocean acidification. *Science*, 318(5857), 1737-1742.
- Hofmann, E., Wrench, P. M., Sharples, F. P., Hiller, R. G., Welte, W., & Diederichs, K. (1996). Structural basis of light harvesting by carotenoids: peridinin-chlorophyll-protein from *Amphidinium carterae*. *Science*, 272(5269), 1788-1791.

- Howe-Kerr, L. I., Bachelot, B., Wright, R. M., Kenkel, C. D., Bay, L. K., & Correa, A. M. (2020). Symbiont community diversity is more variable in corals that respond poorly to stress. *Global Change Biology*, 26(4), 2220-2234.
- Huang, Y., Baxter, R., Smith, B. S., Partch, C. L., Colbert, C. L., & Deisenhofer, J. (2006). Crystal structure of cryptochrome 3 from *Arabidopsis thaliana* and its implications for photolyase activity. *Proceedings of the National Academy of Sciences*, 103(47), 17701-17706.
- Hughes, T. P., Baird, A. H., Dinsdale, E. A., Moltschaniwskyj, N. A., Pratchett, M. S., Tanner, J. E., & Willis, B. L. (2012). Assembly rules of reef corals are flexible along a steep climatic gradient. *Current Biology*, 22(8), 736-741.
- Hughes, T. P., Barnes, M. L., Bellwood, D. R., Cinner, J. E., Cumming, G. S., & Jackson, J. B. C. (2017a). J. 256 Kleypas, IA van de Leemput, JM Lough, TH Morrison, SR Palumbi, EH van Nes, M. 257 Scheffer. *Coral reefs in the Anthropocene*. *Nature*, 546, 82-90.
- Hughes, T. P., Kerry, J. T., Álvarez-Noriega, M., Álvarez-Romero, J. G., Anderson, K. D., Baird, A. H., ... & Wilson, S. K. (2017). Global warming and recurrent mass bleaching of corals. *Nature*, 543(7645), 373-377.
- Hume, B. C., Smith, E. G., Ziegler, M., Warrington, H. J., Burt, J. A., LaJeunesse, T. C., ... & Voolstra, C. R. (2019). SymPortal: A novel analytical framework and platform for coral algal symbiont next-generation sequencing ITS2 profiling. *Molecular ecology resources*, 19(4), 1063-1080.
- Iglesias-Prieto, R., Govind, N. S., & Trench, R. K. (1993). Isolation and characterization of three membranebound chlorophyll-protein complexes from four dinoflagellate species. *Philosophical Transactions of the Royal Society of London. Series B: Biological Sciences*, 340(1294), 381-392.
- IPCC, 2021: Arias, P., Bellouin, N., Coppola, E., Jones, R., Krinner, G., Marotzke, J., ... & Zickfeld, K. (2021). Climate Change 2021: The Physical Science Basis. Contribution of Working Group 14 I to the Sixth Assessment Report of the Intergovernmental Panel on Climate Change; Technical Summary.
- IPCC, 2021 Coral Reefs: Magnan, A. K., Pörtner, H. O., Duvat, V. K., Garschagen, M., Guinder, V. A., Zommers, Z., ... & Gattuso, J. P. (2021). Estimating the global risk of anthropogenic climate change. *Nature climate change*, 11(10), 879-885.
- IUCN. Aeby, G., Lovell, E., Richards, Z., Delbeek, J.C., Reboton, C. & Bass, D. 2008. *Acropora pulchra*. *The IUCN Red List of Threatened Species* 2008: e.T133033A3564383. <https://dx.doi.org/10.2305/IUCN.UK.2008.RLTS.T133033A3564383.en>.

- IUCN. Hoeksema, B.W., Rogers, A. & Quibilan, M.C. 2014. *Pocillopora damicornis*. *The IUCN Red List of Threatened Species* 2014: e.T133222A54216898. <https://dx.doi.org/10.2305/IUCN.UK.2014-1.RLTS.T133222A54216898.en>.
- IUCN. Hoeksema, B.W., Rogers, A. & Quibilan, M.C. 2014. *Pavona decussata*. *The IUCN Red List of Threatened Species* 2014: e.T133041A54183041. <https://dx.doi.org/10.2305/IUCN.UK.2014-1.RLTS.T133041A54183041.en>.
- Jackson, J. B. (1992). Pleistocene perspectives on coral reef community structure. *American Zoologist*, 32(6), 719-731.
- Jandang, S., Viyakarn, V., Yoshioka, Y., Shinzato, C., & Chavanich, S. (2022). The seasonal investigation of Symbiodiniaceae in broadcast spawning, *Acropora humilis* and brooding, *Pocillopora* cf. *damicornis* corals. *PeerJ*, 10, e13114.
- Jiang, J., Zhang, H., Orf, G. S., Lu, Y., Xu, W., Harrington, L. B., ... & Blankenship, R. E. (2014). Evidence of functional trimeric chlorophyll a/c2-peridinin proteins in the dinoflagellate Symbiodinium. *Biochimica et Biophysica Acta (BBA)-Bioenergetics*, 1837(11), 1904-1912.
- Janknegt, P. J., De Graaff, C. M., Van de Poll, W. H., Visser, R. J., Rijstenbil, J. W., & Buma, A. G. (2009). Short-term antioxidative responses of 15 microalgae exposed to excessive irradiance including ultraviolet radiation. *European Journal of Phycology*, 44(4), 525-539.
- Johnson ME, Lustic E, Bartels E, Baums I, Gilliam DS, Learson L, Lirman D, Miller MW, Nedinmayer K, Schopmeyer S, Lustic C, Bartels E, Baums I, Gilliam DS, Larson L, Lirman D, Miller MW, Nedimyer K, Schopmeyer S (2011) Caribbean *Acropora* Restoration Guide: Best Practices for Propagation and Population Enhancement. The Nature Conservancy. 54 pp.
- Jones, A. M., Berkelmans, R., van Oppen, M. J., Mieog, J. C., & Sinclair, W. (2008). A community change in the algal endosymbionts of a scleractinian coral following a natural bleaching event: field evidence of acclimatization. *Proceedings of the Royal Society B: Biological Sciences*, 275(1641), 1359-1365.
- Kagatani, K., Nagao, R., Shen, J. R., Yamano, Y., Takaichi, S., & Akimoto, S. (2022). Excitation relaxation dynamics of carotenoids constituting the diadinoxanthin cycle. *Photosynthesis research*, 154(1), 13-19.
- Kayanne, H., Ishii, T., Matsumoto, E., & Yonekura, N. (1993). Late Holocene sea-level change on Rota and Guam, Mariana Islands, and its constraint on geophysical predictions. *Quaternary Research*, 40(2), 189-200.
- Kisten, Y. (2013). *The influence of heterotrophy on the resilience of hard coral Pocillopora damicornis to thermal stress and bleaching* (Doctoral dissertation).

- Kolari, P., Chan, T., Porcar-Castell, A., Bäck, J., Nikinmaa, E., & Juurola, E. (2014). Field and controlled environment measurements show strong seasonal acclimation in photosynthesis and respiration potential in boreal Scots pine. *Frontiers in plant science*, 5, 717.
- Koornneef, M., Rolff, E., & Spruit, C. J. P. (1980). Genetic control of lightinhibited hypocotyl elongation in *Arabidopsis thaliana* (L.) Heynh. *Z Pflanzenphysiol* 100: 147–160.
- Krediet CJ, DeNofrio JC, Caruso C, Burriesci MS, Cella K, Pringle JR (2015) Rapid, Precise, and Accurate Counts of *Symbiodinium* Cells Using the Guava Flow Cytometer, and a Comparison to Other Methods. *PLoS One* 10(8):e0135725.
- Kuffner, I. B., & Toth, L. T. (2016). A geological perspective on the degradation and conservation of western Atlantic coral reefs. *Conservation Biology*, 30(4), 706-715.
- Kühlbrandt, W., Wang, D. N., & Fujiyoshi, Y. (1994). Atomic model of plant light-harvesting complex by electron crystallography. *Nature*, 367(6464), 614-621.
- LaJeunesse, T. C., Parkinson, J. E., Gabrielson, P. W., Jeong, H. J., Reimer, J. D., Voolstra, C. R., & Santos, S. R. (2018). Systematic revision of Symbiodiniaceae highlights the antiquity and diversity of coral endosymbionts. *Current Biology*, 28(16), 2570-2580.
- LaJeunesse, T. C., Pettay, D. T., Sampayo, E. M., Phongsuwan, N., Brown, B., Obura, D. O., ... & Fitt, W. K. (2010a). Long-standing environmental conditions, geographic isolation and host–symbiont specificity influence the relative ecological dominance and genetic diversification of coral endosymbionts in the genus *Symbiodinium*. *Journal of Biogeography*, 37(5), 785-800.
- LaJeunesse, T. C., Smith, R., Walther, M., Pinzón, J., Pettay, D. T., McGinley, M., ... & Warner, M. E. (2010b). Host–symbiont recombination versus natural selection in the response of coral–dinoflagellate symbioses to environmental disturbance. *Proceedings of the Royal Society B: Biological Sciences*, 277(1696), 2925-2934.
- LaJeunesse, T. C., Thornhill, D. J., Cox, E. F., Stanton, F. G., Fitt, W. K., & Schmidt, G. W. (2004). High diversity and host specificity observed among symbiotic dinoflagellates in reef coral communities from Hawaii. *Coral reefs*, 23(4), 596-603.
- LaJeunesse, T. C., Wham, D. C., Pettay, D. T., Parkinson, J. E., Keshavmurthy, S., & Chen, C. A. (2014). Ecologically differentiated stress-tolerant endosymbionts in the dinoflagellate genus *Symbiodinium* (Dinophyceae) Clade D are different species. *Phycologia*, 53(4), 305-319.

- LaJeunesse, T. C. (2005). "Species" radiations of symbiotic dinoflagellates in the Atlantic and Indo-Pacific since the Miocene-Pliocene transition. *Molecular biology and evolution*, 22(3), 570-581.
- Lavaud, J., and Goss, R. (2014) The peculiar features of nonphotochemical fluorescence quenching in diatoms and brown algae. In *Non-Photochemical Quenching and Energy Dissipation in Plants, Algae and Cyanobacteria*. Demmig-Adams, B., Garab, G., III, and Govindjee, W.A. (eds). Springer: New York. pp. 421–443.
- Lee, J., Song, J., Lee, D., & Pang, Y. (2019). Metal-enhanced fluorescence and excited state dynamics of carotenoids in thin polymer films. *Scientific Reports*, 9(1), 3551.
- Loya, Y. (1976). Recolonization of Red Sea corals affected by natural catastrophes and manmade perturbations. *Ecology*, 57(2), 278-289.
- Mäkelä, A., Hari, P., Berninger, F., Hänninen, H., & Nikinmaa, E. (2004). Acclimation of photosynthetic capacity in Scots pine to the annual cycle of temperature. *Tree physiology*, 24(4), 369-376.
- Matthews, J. L., Crowder, C. M., Oakley, C. A., Lutz, A., Roessner, U., Meyer, E., ... & Davy, S. K. (2017). Optimal nutrient exchange and immune responses operate in partner specificity in the cnidarian-dinoflagellate symbiosis. *Proceedings of the National Academy of Sciences*, 114(50), 13194-13199.
- Martinez Arbizu P (2017) pairwiseAdonis: Pairwise Multilevel Comparison using Adonis. R package version 0.4.
- McClanahan, T. R. (2008). Response of the coral reef benthos and herbivory to fishery closure management and the 1998 ENSO disturbance. *Oecologia*, 155(1), 169-177.
- McClanahan, T. R. (2004). The relationship between bleaching and mortality of common corals. *Marine Biology*, 144(6), 1239-1245.
- Menne, M.J., I. Durre, B. Korzeniewski, S. McNeill, K. Thomas, X. Yin, S. Anthony, R. Ray, R.S. Vose, B.E. Gleason, and T.G. Houston, 2012: Global Historical Climatology Network - Daily (GHCN-Daily), Version 3. NOAA National Climatic Data Center
- Mezaki, T., Keshavmurthy, S., & Chen, C. A. (2014). An old and massive colony of *Pavona decussata* is sexually active at high latitude (32° N) in Japan. *Coral Reefs*, 33(1), 97-97.
- Mote, S., Gupta, V., De, K., Hussain, A., More, K., Nanajkar, M., & Ingole, B. (2021). Differential Symbiodiniaceae association with coral and coral-eroding sponge in a bleaching Impacted marginal coral reef environment. *Frontiers in Marine Science*, 8, 666825.

- Mukherjee, A., Walker, J., Weyant, K. B., & Schroeder, C. M. (2013). Characterization of flavin-based fluorescent proteins: an emerging class of fluorescent reporters. *PLoS one*, 8(5), e64753.
- Muller, E. M., Bartels, E., & Baums, I. B. (2018). Bleaching causes loss of disease resistance within the threatened coral species *Acropora cervicornis*. *Elife*, 7.
- Murage, E. N., & Masuda, M. (1997). Response of pepper and eggplant to continuous light in relation to leaf chlorosis and activities of antioxidative enzymes. *Scientia horticulturae*, 70(4), 269-279.
- Muscatine, L. E. O. N. A. R. D., & Porter, J. W. (1977). Reef corals: mutualistic symbioses adapted to nutrient-poor environments. *Bioscience*, 27(7), 454-460.
- Muscatine, L., Falkowski, P. G., Porter, J. W., & Dubinsky, Z. (1984). Fate of photosynthetic fixed carbon in light-and shade-adapted colonies of the symbiotic coral *Stylophora pistillata*. *Proceedings of the Royal Society of London. Series B. Biological Sciences*, 222(1227), 181-202.
- Nakamura, T. V., (2010). Importance of water-flow on the physiological responses of reef-building corals. *Galaxea, Journal of Coral Reef Studies*, 12(1), 1-14.
- Nakamura, T. V., & Van Woesik, R. (2001). Water-flow rates and passive diffusion partially explain differential survival of corals during the 1998 bleaching event. *Marine Ecology Progress Series*, 212, 301-304.
- Niedzwiedzki, D. M., Jiang, J., Lo, C. S., & Blankenship, R. E. (2014). Spectroscopic properties of the Chlorophyll a–Chlorophyll c 2–Peridinin-Protein-Complex (acpPC) from the coral symbiotic dinoflagellate *Symbiodinium*. *Photosynthesis research*, 120(1), 125-139.
- Niyogi, K.K. (1999) Photoprotection Revisited: Genetic and Molecular Approaches. *Annual Review of Plant Physiology and Plant Molecular Biology*, 50, 333-359. <http://dx.doi.org/10.1146/annurev.arplant.50.1.333>
- Norris, B. J., & Miller, D. J. (1994). Nucleotide sequence of a cDNA clone encoding the precursor of the peridinin-chlorophyll a-binding protein from the dinoflagellate *Symbiodinium* sp. *Plant molecular biology*, 24(4), 673-677.
- Odum, E. P. (1969). The Strategy of Ecosystem Development: An understanding of ecological succession provides a basis for resolving man's conflict with nature. *science*, 164(3877), 262-270.
- Oksanen J, Blanchet FG, Friendly M, Kindt R, Legendre P, Minchin PR, Wagner H (2019) *Vegan: Community Ecology Package*. R package version 2.5–6. <https://CRAN.Rproject.org/package=vegan>

- Okubo, N., Mezaki, T., Nozawa, Y., Nakano, Y., Lien, Y. T., Fukami, H., ... & Ball, E. E. (2013). Comparative embryology of eleven species of stony corals (Scleractinia). *PLoS One*, 8(12), e84115.
- Oliver, T. A., & Palumbi, S. R. (2011). Do fluctuating temperature environments elevate coral thermal tolerance?. *Coral reefs*, 30(2), 429-440.
- Osinga, R., Derksen-Hooijberg, M., Wijgerde, T., & Verreth, J. A. (2017). Interactive effects of oxygen, carbon dioxide and flow on photosynthesis and respiration in the scleractinian coral *Galaxea fascicularis*. *Journal of Experimental Biology*, 220(12), 2236-2242.
- Pandolfi, J. M., & Jackson, J. B. (2006). Ecological persistence interrupted in Caribbean coral reefs. *Ecology Letters*, 9(7), 818-826.
- Perumal, S. S., Shanthi, P., & Sachdanandam, P. (2005). Augmented efficacy of tamoxifen in rat breast tumorigenesis when gavaged along with riboflavin, niacin, and CoQ10: effects on lipid peroxidation and antioxidants in mitochondria. *Chemico-biological interactions*, 152(1), 49-58.
- Pokorny, R., Klar, T., Hennecke, U., Carell, T., Batschauer, A., & Essen, L. O. (2008). Recognition and repair of UV lesions in loop structures of duplex DNA by DASH-type cryptochrome. *Proceedings of the National Academy of Sciences*, 105(52), 21023-21027.
- Polívka, T., Hiller, R. G., & Frank, H. A. (2007). Spectroscopy of the peridinin-chlorophyll-a protein: insight into light-harvesting strategy of marine algae. *Archives of biochemistry and biophysics*, 458(2), 111-120.
- Polívka, T., Van Stokkum, I. H., Zigmantas, D., Van Grondelle, R., Sundström, V., & Hiller, R. G. (2006). Energy transfer in the major intrinsic light-harvesting complex from *Amphidinium carterae*. *Biochemistry*, 45(28), 8516-8526.
- Porcar-Castell, A., Juurola, E., Ensminger, I., Berninger, F., Hari, P., & Nikinmaa, E. (2008). Seasonal acclimation of photosystem II in *Pinus sylvestris*. II. Using the rate constants of sustained thermal energy dissipation and photochemistry to study the effect of the light environment. *Tree physiology*, 28(10), 1483-1491.
- Qin, Z., Yu, K., Chen, B., Wang, Y., Liang, J., Luo, W., ... & Huang, X. (2019). Diversity of Symbiodiniaceae in 15 coral species from the southern South China

Sea: potential relationship with coral thermal adaptability. *Frontiers in Microbiology*, 10, 2343.

- R Core Team. (2022). R: A language and environment for statistical computing. R Foundation for Statistical Computing, Vienna, Austria. <https://www.R-project.org/>
- Ramel, F., Birtic, S., Ginies, C., Soubigou-Taconnat, L., Triantaphylidès, C., & Havaux, M. (2012). Carotenoid oxidation products are stress signals that mediate gene responses to singlet oxygen in plants. *Proceedings of the National Academy of Sciences*, 109(14), 5535-5540.
- Randall, R. H. (1979). *Geologic features within the Guam seashore study area*. University of Guam Marine Laboratory.
- Randall, R. H., & Eldredge, L. G. (1977). Life on Guam: Coral Reef.
- Raymundo, L. J., Burdick, D., Lapacek, V. A., Miller, R., & Brown, V. (2017). Anomalous temperatures and extreme tides: Guam staghorn Acropora succumb to a double threat. *Marine Ecology Progress Series*, 564, 47-55.
- Raymundo, L. J., Burdick, D., Hoot, W. C., Miller, R. M., Brown, V., Reynolds, T., ... & Williams, A. (2019). Successive bleaching events cause mass coral mortality in Guam, Micronesia. *Coral Reefs*, 38(4), 677-700.
- Raymundo LJ, Anderson MD, Moreland-Ochoa C, Castro A, Lock C, Burns N, Tajjeron F, Combosch D, Burdick D. (2022) Conservation and Active Restoration of Guam's Staghorn Acropora Corals. Report #168, University of Guam Marine Laboratory.
- Richmond, R. H., & Hunter, C. L. (1990). Reproduction and recruitment of corals: comparisons among the Caribbean, the tropical Pacific, and the Red Sea. *Marine ecology progress series. Oldendorf*, 60(1), 185-203.
- Rodgers, S. K., Bahr, K. D., Jokiel, P. L., & Donà, A. R. (2017). Patterns of bleaching and mortality following widespread warming events in 2014 and 2015 at the Hanauma Bay Nature Preserve, Hawai 'i. *PeerJ*, 5, e3355.
- Roff, G., Clark, T. R., Reymond, C. E., Zhao, J. X., Feng, Y., McCook, L. J., ... & Pandolfi, J. M. (2013). Palaeoecological evidence of a historical collapse of corals at Pelorus Island, inshore Great Barrier Reef, following European settlement. *Proceedings of the Royal Society B: Biological Sciences*, 280(1750), 20122100.

- Rowan, R., Knowlton, N., Baker, A., & Jara, J. (1997). Landscape ecology of algal symbionts creates variation in episodes of coral bleaching. *Nature*, *388*(6639), 265-269.
- Rowan, R. O. B., & Powers, D. A. (1991). A molecular genetic classification of zooxanthellae and the evolution of animal-algal symbioses. *Science*, *251*(4999), 1348-1351.
- Rowan, R., & Powers, D. A. (1992). Ribosomal RNA sequences and the diversity of symbiotic dinoflagellates (zooxanthellae). *Proceedings of the National Academy of Sciences*, *89*(8), 3639-3643.
- RStudio Team (2022) RStudio: Integrated Development for R. RStudio, PBC, Boston, MA. <http://www.rstudio.com/>
- Safaie, A., Silbiger, N. J., McClanahan, T. R., Pawlak, G., Barshis, D. J., Hench, J. L., ... & Davis, K. A. (2018). High frequency temperature variability reduces the risk of coral bleaching. *Nature communications*, *9*(1), 1671.
- Sampayo, E. M., Franceschinis, L., Hoegh-Guldberg, O. V. E., & Dove, S. (2007). Niche partitioning of closely related symbiotic dinoflagellates. *Molecular ecology*, *16*(17), 3721-3733.
- Sancar, A. (1994). Structure and function of DNA photolyase. *Biochemistry*, *33*(1), 2-9.
- Sandin, S. A., & Sala, E. (2012). Using successional theory to measure marine ecosystem health. *Evolutionary Ecology*, *26*(2), 435-448.
- Schmidt-Roach, S., Lundgren, P., Miller, K. J., Gerlach, G., Noreen, A. M., & Andreakis, N. (2013). Assessing hidden species diversity in the coral *Pocillopora damicornis* from Eastern Australia. *Coral Reefs*, *32*(1), 161-172.
- Schmidt-Roach, S., Miller, K. J., Woolsey, E., Gerlach, G., & Baird, A. H. (2012). Broadcast spawning by *Pocillopora* species on the Great Barrier Reef. *PLoS One*, *7*(12), e50847.
- Shalitin, D., Yang, H. Y., Mockler, T. C., Maymon, M., Guo, H. W., Whitelam, G. C., & Lin, C. T. (2002). Regulation of *Arabidopsis* cryptochrome 2 by blue-light-dependent phosphorylation.[Erratum: July 25, 2002, v. 418 (6896), p. 447.].
- Sharma, P., Jha, A.B., Dubey, R.S., and Pessarakli, M. (2012) Reactive oxygen species, oxidative damage, and antioxidative defense mechanism in plants under stressful conditions. *J Bot* 1–26.
- Shick, J. M., Lesser, M. P., & Jokiel, P. L. (1996). Effects of ultraviolet radiation on corals and other coral reef organisms. *Global Change Biology*, *2*(6), 527-545.

- Shumbe, L., Bott, R., & Havaux, M. (2014). Dihydroactinidiolide, a high light-induced β -carotene derivative that can regulate gene expression and photoacclimation in *Arabidopsis*. *Molecular Plant*, 7(7), 1248-1251.
- Siefermann-Harms, D., Joyard, J., & Douce, R. (1978). Light-induced changes of the carotenoid levels in chloroplast envelopes. *Plant physiology*, 61(4), 530-533.
- Siegrist Jr, H. G., Randall, R. H., & Siegrist, A. W. (1984). Petrography of the Merizo limestone, an emergent Holocene reef, Ylig Point, Guam. *Palaeontographica Americana*, 54, 399-405.
- Silverstein, R. N., Cunning, R., & Baker, A. C. (2017). Tenacious D: Symbiodinium in clade D remain in reef corals at both high and low temperature extremes despite impairment. *Journal of Experimental Biology*, 220(7), 1192-1196.
- Slavov, C., Schrameyer, V., Reus, M., Ralph, P. J., Hill, R., Büchel, C., ... & Holzwarth, A. R. (2016). "Super-quenching" state protects Symbiodinium from thermal stress—implications for coral bleaching. *Biochimica Et Biophysica Acta (BBA)-Bioenergetics*, 1857(6), 840-847.
- Small, G. D., Min, B., & Lefebvre, P. A. (1995). Characterization of a *Chlamydomonas reinhardtii* gene encoding a protein of the DNA photolyase/blue light photoreceptor family. *Plant molecular biology*, 28(3), 443-454.
- Smerilli, A., Orefice, I., Corato, F., Gavalás Olea, A., Ruban, A. V., & Brunet, C. (2017). Photoprotective and antioxidant responses to light spectrum and intensity variations in the coastal diatom *Skeletonema marinoi*. *Environmental microbiology*, 19(2), 611-627.
- Smith, L. W., & Birkeland, C. (2007). Effects of intermittent flow and irradiance level on back reef *Porites* corals at elevated seawater temperatures. *Journal of Experimental Marine Biology and Ecology*, 341(2), 282-294.
- Song, P. S., Koka, P., Prezelin, B. B., & Haxo, F. T. (1976). Molecular topology of the photosynthetic light-harvesting pigment complex, peridinin-chlorophyll a-protein, from marine dinoflagellates. *Biochemistry*, 15(20), 4422-4427.
- Stimson, J., Sakai, K., & Sembali, H. (2002). Interspecific comparison of the symbiotic relationship in corals with high and low rates of bleaching-induced mortality. *Coral reefs*, 21, 409-421.
- Sully, S., Burkepile, D. E., Donovan, M. K., Hodgson, G., & Van Woesik, R. (2019). A global analysis of coral bleaching over the past two decades. *Nature communications*, 10(1), 1-5.
- Swapnil, P., Meena, M., Singh, S. K., Dhuldhaj, U. P., & Marwal, A. (2021). Vital roles of carotenoids in plants and humans to deteriorate stress with its structure,

- biosynthesis, metabolic engineering and functional aspects. *Current Plant Biology*, 26, 100203.
- Taboroši, D., Jenson, J. W., & Mylroie, J. E. (2004). *Karst Features of Guam Mariana Islands*. Water and Environmental Research Institute of the Western Pacific, University of Guam.
- Taheri, P., & Tarighi, S. (2010). Riboflavin induces resistance in rice against *Rhizoctonia solani* via jasmonate-mediated priming of phenylpropanoid pathway. *Journal of plant physiology*, 167(3), 201-208.
- Tamai, T. K., Young, L. C., & Whitmore, D. (2007). Light signaling to the zebrafish circadian clock by Cryptochrome 1a. *Proceedings of the National Academy of Sciences*, 104(37), 14712-14717.
- Taylor, F. W., Jouannic, C., & Bloom, A. L. (1985). Quaternary uplift of the Torres Islands, northern New Hebrides frontal arc: Comparison with Santo and Malekula Islands, central New Hebrides frontal arc. *The Journal of Geology*, 93(4), 419-438.
- Toh, T. C., Peh, J. W. K., & Chou, L. M. (2013). Heterotrophy in recruits of the scleractinian coral *Pocillopora damicornis*. *Marine and Freshwater Behaviour and Physiology*, 46(5), 313-320.
- Van Gelder, R. N., Wee, R., Lee, J. A., & Tu, D. C. (2003). Reduced pupillary light responses in mice lacking cryptochromes. *Science*, 299(5604), 222-222.
- Van Riel, M., Hammans, J. K., Van De Ven, M., Verwer, W., & Levine, Y. K. (1983). Fluorescence excitation profiles of beta-carotene in solution and in lipid/water mixtures. *Biochemical and Biophysical Research Communications*, 113(1), 102-107.
- Vega Thurber, R. L., Burkepile, D. E., Fuchs, C., Shantz, A. A., McMinds, R., & Zaneveld, J. R. (2014). Chronic nutrient enrichment increases prevalence and severity of coral disease and bleaching. *Global change biology*, 20(2), 544-554.
- Veron J. E. N.. (1986). *Corals of Australia and the Indo-Pacific*. Angus & Robertson Publishers.
- Walker, L. R., & Del Moral, R. (2003). *Primary succession and ecosystem rehabilitation*. Cambridge University Press.
- Ward, S. (1992). Evidence for broadcast spawning as well as brooding in the scleractinian coral *Pocillopora damicornis*. *Marine Biology*, 112(4), 641-646.
- Warner, M. E., Fitt, W. K., & Schmidt, G. W. (1999). Damage to photosystem II in symbiotic dinoflagellates: a determinant of coral bleaching. *Proceedings of the National Academy of Sciences*, 96(14), 8007-8012.

- Wepfer, P. H., Nakajima, Y., Hui, F. K., Mitarai, S., & Economo, E. P. (2020). Metacommunity ecology of Symbiodiniaceae hosted by the coral *Galaxea fascicularis*. *Marine Ecology Progress Series*, 633, 71-87.
- Wickham H (2016) *ggplot2: Elegant Graphics for Data Analysis*. Springer New York.
- Widiastuti K, Azadeh S, Ross H, Wah SC, Jun M, Michio H, Shunichi T (2015). Novel characteristics of photodamage to PS II in a high-light-sensitive Symbiodinium phylotype. *Plant Cell Physiol* 56:1162–1171
- Yonge and Nichols, B. M. Natural, & Expedition, G. B. R. (1931). *Scientific Reports / Great Barrier Reef Expedition 1928-29.: Vol. v.1(1930-1940)*. BM(NH). <https://www.biodiversitylibrary.org/item/136859>
- Yu, X., Yu, K., Liao, Z., Liang, J., Deng, C., Huang, W., & Huang, Y. (2020). Potential molecular traits underlying environmental tolerance of *Pavona decussata* and *Acropora pruinosa* in Weizhou Island, northern South China Sea. *Marine Pollution Bulletin*, 156, 111199.
- Yuyama, I., Ishikawa, M., Nozawa, M., Yoshida, M. A., & Ikeo, K. (2018). Transcriptomic changes with increasing algal symbiont reveal the detailed process underlying establishment of coral-algal symbiosis. *Scientific reports*, 8(1), 16802.

Appendix

Table 1A: Peridinin – Chlorophyll LHC linear models specific to site, species, and time.

Time	Site	Species	R²	Corr	Slope
February (T1)	Tanguisson	<i>Acropora pulchra</i>	0.922	0.960	0.750
	Tanguisson	<i>Pocillopora damicornis</i>	0.886	0.940	1.240
	Tanguisson	<i>Pavona decussata</i>	0.490	0.700	2.130
	West Agaña	<i>Acropora pulchra</i>	0.168	0.410	0.140
	West Agaña	<i>Pocillopora damicornis</i>	0.860	0.930	1.750
	West Agaña	<i>Pavona decussata</i>	0.743	0.860	0.310
May (T2)	Tanguisson	<i>Acropora pulchra</i>	0.645	0.800	0.579
	Tanguisson	<i>Pocillopora damicornis</i>	0.698	0.840	0.876
	Tanguisson	<i>Pavona decussata</i>	0.668	0.820	0.995
	West Agaña	<i>Acropora pulchra</i>	0.123	-0.350	-0.273
	West Agaña	<i>Pocillopora damicornis</i>	0.541	0.740	1.391
	West Agaña	<i>Pavona decussata</i>	0.355	0.600	0.680
August (T3)	Tanguisson	<i>Acropora pulchra</i>	0.823	0.910	1.430
	Tanguisson	<i>Pocillopora damicornis</i>	0.754	-0.870	0.614
	Tanguisson	<i>Pavona decussata</i>	0.729	0.850	1.312
	West Agaña	<i>Acropora pulchra</i>	0.340	0.580	1.042
	West Agaña	<i>Pocillopora damicornis</i>	0.036	-0.190	-0.090
	West Agaña	<i>Pavona decussata</i>	0.272	0.520	0.371
November (T4)	Tanguisson	<i>Acropora pulchra</i>	0.079	0.280	0.551
	Tanguisson	<i>Pocillopora damicornis</i>	0.477	0.690	0.493
	Tanguisson	<i>Pavona decussata</i>	0.261	0.510	0.652
	West Agaña	<i>Acropora pulchra</i>	0.724	0.850	1.104
	West Agaña	<i>Pocillopora damicornis</i>	0.007	0.090	0.061
	West Agaña	<i>Pavona decussata</i>	0.558	0.750	0.730

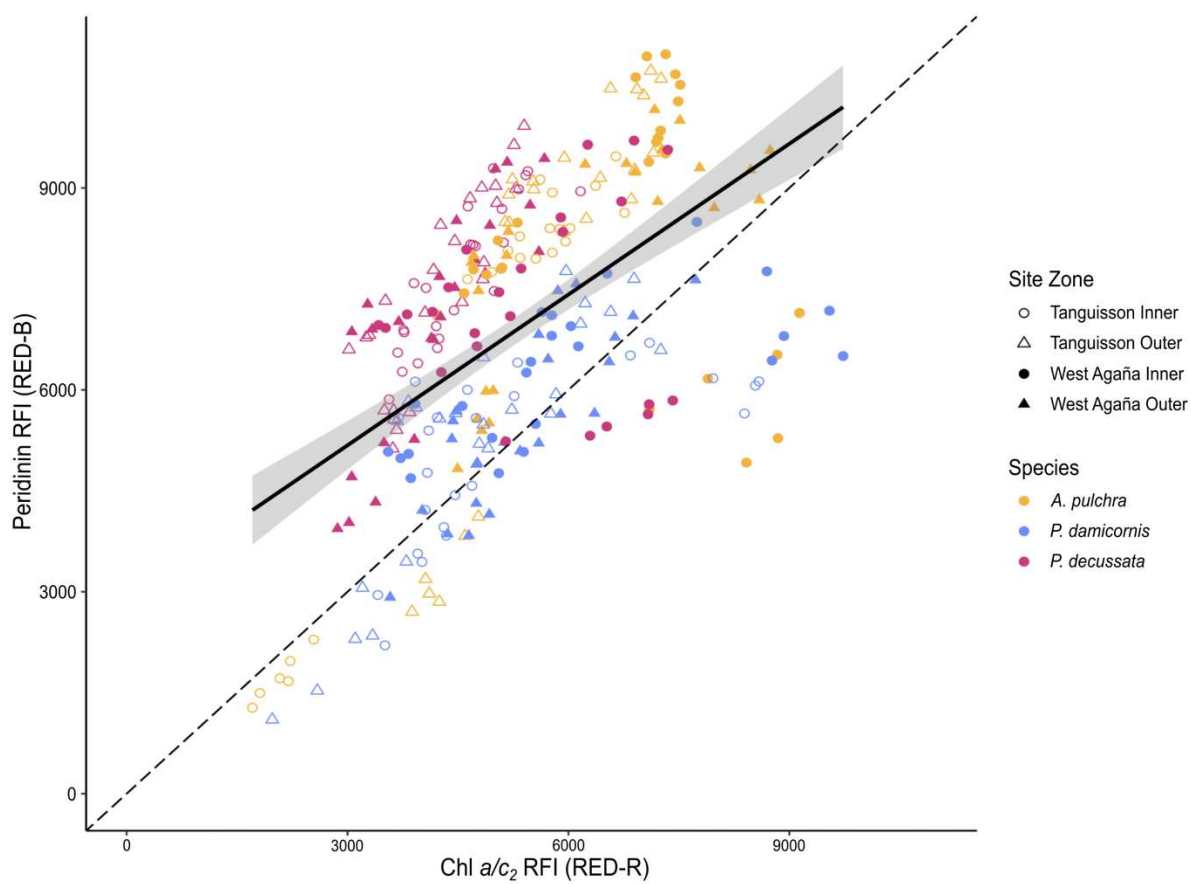


Figure 1A: Linear regression model pooled by time (February, May, August, November), site (Tanguisson, West Agaña), zone (Inner, Outer), and species (*Acropora pulchra*, *Pocillopora damicornis*, *Pavona decussata*) revealing near 1:1 peridinin-chlorophyll ratio.



Figure 2A: Algal growth on *Acropora pulchra* tips after extreme low tides exposed *A. pulchra*. Taken at the West Agaña site in August of 2022.

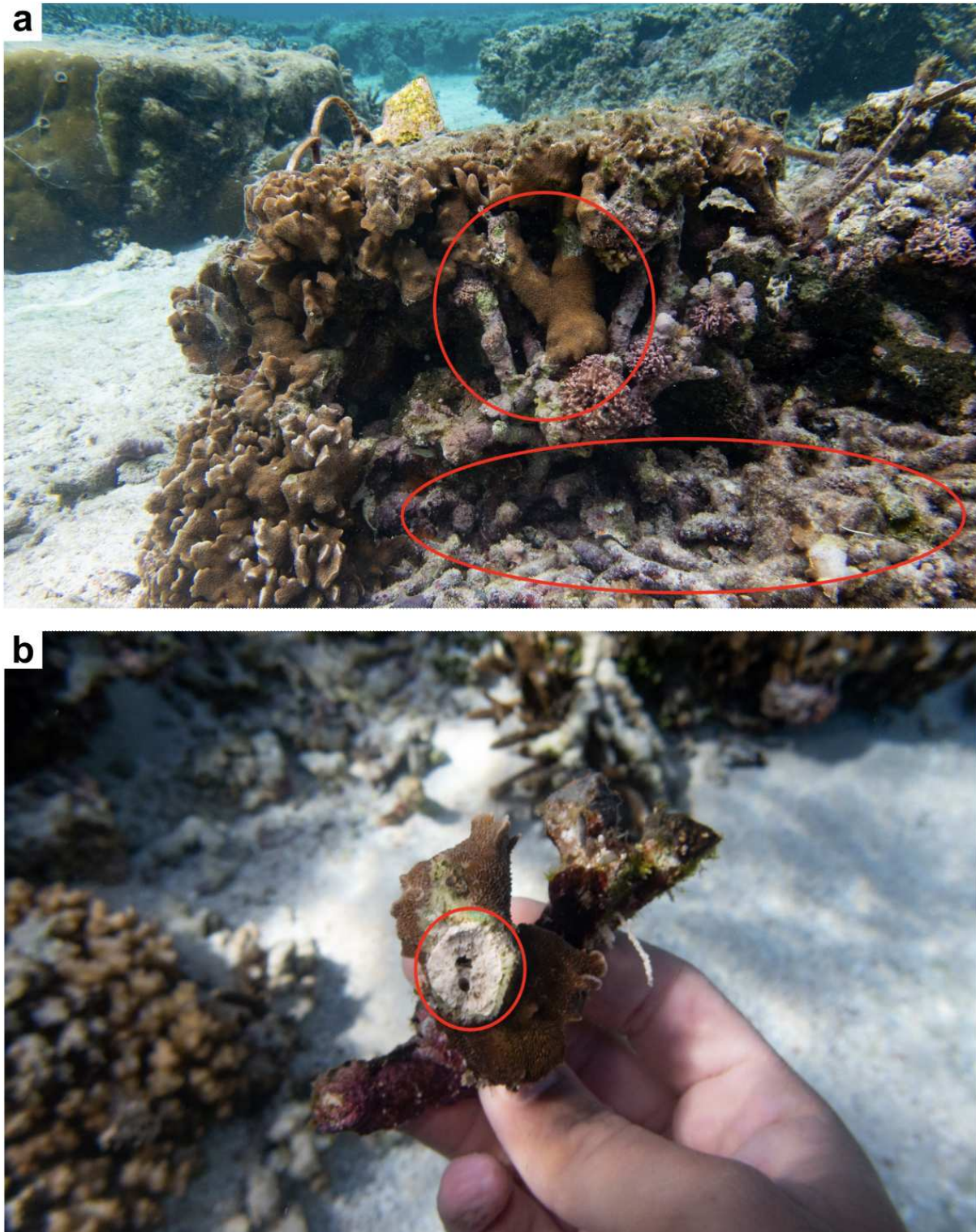


Figure 3A: Historical evidence of species replacements on Guam's reef flats **a)** *Pavona decussata* growing over a branching growth form next to dead *Acropora* rubble **b)** Cross section of dead *Acropora* overgrown by live *Pavona decussata*.

